國立交通大學

生物科技研究所

碩 士 論 文

大腸桿菌表現 *Coprinus cinereus* 過氧化氫酵素之特性研究

Characterization of Bacterial Expressed Recombinant *Coprinus cinereus* Peroxidase

研 究 生：王俊能

指導教授：袁俊傑　博士

中 華 民 國 九 十 七 年 七 月

大腸桿菌表現 *Coprinus cinereus* 過氧化氫酵素之特性研究

Characterization of Bacterial Expressed Recombinant *Coprinus cinereus* Peroxidase

研 究 生：王俊能　　Student：Chun-Neng Wang

指導教授：袁俊傑 博士　　Advisor：Dr. Chiun-Jye Yuan

國 立 交 通 大 學

生 物 科 技 研 究 所

碩 士 論 文

A Thesis

Submitted to Institute of Biological Science and Technology

National Chiao Tung University

In Partial Fulfillment of the Requirements

for the Degree of

Master

In

Biological Science and Technology

July 2008

Hsinchu, Taiwan, Republic of China

中華民國九十七年七月

大腸桿菌表現 *Coprinus cinereus* 過氧化氫酵素之特性研究

學生：王俊能　　指導教授：袁俊傑博士

國立交通大學生物科技研究所碩士論文

中文摘要

Coprinus cinereus peroxidase (CIP) 為含血基質的過氧化氫酵素，可在過氧化氫存在下將酚類化合物及其衍生物氧化。CIP 於大腸桿菌中表現，其生物物理以及生化特性將被進一步的分析。大腸桿菌表現無醣基化的重組 CIP，其為無活性的包涵體，接著於 4 ℃，1.8 M urea，10 mM $CaCl_2$ 和 5 μM hemin 條件下再摺疊達七小時。具有活性的 CIP 經過純化其產量為 15 %，且經由 2,2'-azino-bis (3-ethylbenzothiazoline -6-sulfonate) (ABTS) 的測定，其比活性為 23544 U/mg。重組 CIP 最適的催化條件為 pH 5 以及 35 ℃。而重組 CIP 的熱穩定性可經由活性分析、UV-Vis 光譜分析、掃描式熱差分儀 (differential scanning calorimetry, DSC)、和旋光光譜儀 (circular dichroism, CD) 等方法來測定。EDTA 可以增加失活的速率，而鈣離子有可逆的影響。在 DSC 實驗顯示熔點 (T_m) 為 48 ℃，去摺疊的熱力學參數為 ΔH_{cal} = 348.3 KJ/mol、ΔS = 1.09 KJ/mol。經 CD 光譜研究證實，溫度高於 55 ℃ 會造成重組 CIP 構形改變。CIP 比 HRP 有較高的催化效率，而其高催化特性在未來的研究是極具潛力的。

Characterization of Bacterial Expressed Recombinant *Coprinus cinereus* Peroxidase

Student: Wang, Chun-Neng Adviser: Dr.Yuan, Chiun-Jye

Department of Biological Science and Technology National Chiao Tung University

Abstract

Coprinus cinereus peroxidase (CIP) is a heme-containing enzyme that oxidizes a wide variety of phenolic compounds and derivatives in the presence of H_2O_2. To further characterize the biophysical and biochemical properties of CIP was overexpressed in *Escherichia coli* BL21 (DE3). The nonglycosylated recombinant CIP was expressed as an inactive inclusion body and subsequent by renatured under 4 ℃ in the presence of 1.8 M urea, 10 mM $CaCl_2$ and 5 μM hemin for 7 h. The yield of active recombinant CIP was about 15 % with the specific activity of 23544 U/mg by using 2,2'-azino-bis (3-ethylbenzothiazoline -6-sulfonate) (ABTS) as substrate. The highest activity could be observed at around pH 5 and 35 ℃. The thermostability of the recombinant CIP were studied by activity assay, UV-Vis spectrophotometer analysis, differential scanning calorimetry (DSC), and circular dichroism (CD). EDTA increased the rate of inactivation, which could be reversed by Ca^{2+} ion. DSC experiments show the transition temperature (T_m) for recombinant CIP is 48 ℃. The enthalpy (ΔH) and entropy (ΔS) of the recombinant CIP in thermal denaturation were calculated as ΔH_{cal} = 348.3 KJ/mol, ΔS = 1.09 KJ/mol/K. Circular dichroism studies prove that temperatures higher than 55 ℃ induced a change in the conformation of the recombinant CIP. CIP exhibits higher catalytic activity than that of HRP, suggesting a potential for future application.

致謝

碩士班生活，終要在此劃下句點，首先要感謝指導教授 袁俊傑老師對我的指導與教誨，雖然在求學期間給老師添了一些麻煩，但還是很感謝老師給我很多機會；感謝口試委員 吳東昆老師 及 黃國柱老師於口試時給予寶貴意見，讓我有不同的思考方向；也感謝 常怡雍老師 及 邱子珍老師在我助理生活給予諸多啟發，讓我獲益匪淺。

也感謝實驗室的成員，在觀念上以及實驗技巧給予很多的幫助。實驗室的學長姐俊炫、 威震、奕榮、君璇、岳縉、元碩、叔青、宜芳、詩穎、世昌、彥棋；還有同學 雯世、偉志；學弟妹 佩琴、君怡、靜如、中亮、義宇，讓我的研究生生活更加充實。此外，也要感謝吳東昆老師實驗室、彭慧玲老師實驗室、張家靖老師實驗室、楊裕雄老師實驗室以及曾幫助過我的每一個人，讓我的實驗能順利的完成。

最後，要感謝我的家人還有曉萍，沒有他們在後面的支持，研究生活勢必會更艱辛與乏味。也謝謝我的朋友們，讓我的生活更多彩多姿。

Contents

Figure contents

Table contents

Abbreviation

CIP	*Coprinus cinereus* peroxidase
ARP	*Arthromyces ramosus* peroxidase
AOPTP	African oil palm tree peroxidase
HRP	Horseradish peroxidase
SBP	Soybean peroxidase
MnP	Manganese peroxidase
PchrMnP	*Phanerochaete chrysosporium* manganese peroxidase
IPTG	Isopropyl-β-thiogalactoside
DTT	Dithiothreitol
DMAB	Dimethylamine borane
GSSG	Oxidized Glutathione
EDTA	Ethylenediaminetetraacetic acid
MBTH	3-methyl-2-benzothiazolinone hydrazone
SDS-PAGE	Sodium dodecyl sulfate -polyacrylamiude gel
4-AAP	4-aminoantipyrine
CD	Circular dichroism
DSC	Differential scanning calorimetry

I. Introduction

I-1 General features of peroxidase

Peroxidases (EC 1.11.1.7) are heme–containing enzymes that act on a wide variety of compounds, such as phenol, and luminol, 2,2'-azino-bis(3-ethylbenzothiazoline-6-sulfonate) (ABTS), in the presence of H_2O_2. Peroxidases play important roles in the animal, plant, and the microorganism. The plant peroxidases participate in the metabolism of auxin which signals growth and development of plants. Peroxidases can oxidize substances of physiological relevance including plant hormones (e.g., indole-3-acetic acid and its derivatives) and lignin precursors (*7*). They also play roles in extracellular defense against pathogens and stress, biosynthesis and degradation of lignin, removal of hydrogen peroxide and oxidation of toxic reductants (*8*).

The plant peroxidase superfamily is divided into three subclasses based on their amino acid sequence homology. The class I subfamily is composed of intracelluar perioxidases including yeast cytochrome c peroxidase, chloroplast and cytosol ascorbate peroxidases. Class I subfamily contains a heme-binding site at their N-terminal domain. Both the fungal peroxidases (Class II) and the class III plant peroxidases are secretory peroxidases that contain an N-terminal signal peptide sequence. The class II subfamily consists of LIP (lignin peroxidase), MnP (manganese peroxidase), and peroxidases from inkcap fungal *Coprinus cinereus* (CIP), containing about 5 % carbohydrates, two calcium ions, and four disulfide bridges . The members of class III subfamily also contain two calcium ions, four conserved disulfide bridges, but with the glycosylation ranges from 0 to 25 %. Class III plant peroxidases also contain extra helices that play a role in access to the heme edge. The horseradish root peroxidase (HRP) and peanut peroxidase are two well known class III plant peroxidases (*9*).

CIP is a monomeric glycoprotein with a molecular weight of 38000 and a pI value of

3.5 (*10*). The carbohydrate content of CIP is approximately 5%. It has been shown that the *A. ramosus* peroxidase (ARP) and the CIP are almost identical in amino acid sequence to each other. A tetraglycine segment in the N-terminal glycine-rich extension of CIP is replaced by a pentaglycine segment in ARP. The degree of N-glycosylation, however, is the only difference between CIP and ARP. Other than that, there is no dramatic difference in the catalytic properties between two peroxidases (*2, 10*).

I-2 Stereostructure of CIP/ARP

The crystal structures of *C. cinereus* (*1, 11*) and *A. ramosus* peroxidases (*12-14*) were solved and reported. CIP is an α-protein consisting of 10 major and two short helices and a few short β-strands. The overall folding of CIP is shown in Fig. I-1. The distal domain (at N-terminal site) contains the helices A, B, B', B'', C, D and E, the helices F, J, H, I and G are part of the proximal domain (at C-terminal site; proximal His183). The J helix connects the two domains and continues in a large loop, extending over the top of the distal domain and goes back to the proximal domain. The only difference in helical topology between CIP and yeast cytochrome C peroxidase (*15*) is two additional helices, B'' and B', between B and C in CIP. The folded structure of CIP is almost identical to that of LIP (*16*) with a few differences in the loop and C-terminal regions . The catalytic activity of the peroxidases is associated with the heme group and conserved catalytic residues in the heme pocket. The catalytically important amino acids in CIP have been identified as Arg51, Phe54, His55, His183 and Asp245 (*1, 17*). His183 , a proximal His, coordinates to the iron in the heme groups; whereas Asp92 forms a bridge between His55 and main chain carbonyl of Glu86 via hydrogen bonds. CIP exhibits a broad substrate specificity with a large opening at its active site. For example, the larger residues in the active site of LIP, e.g., I85, E146, F148 and D183 were replaced with Gly93, G154, G156 and G190 in CIP (*1*).

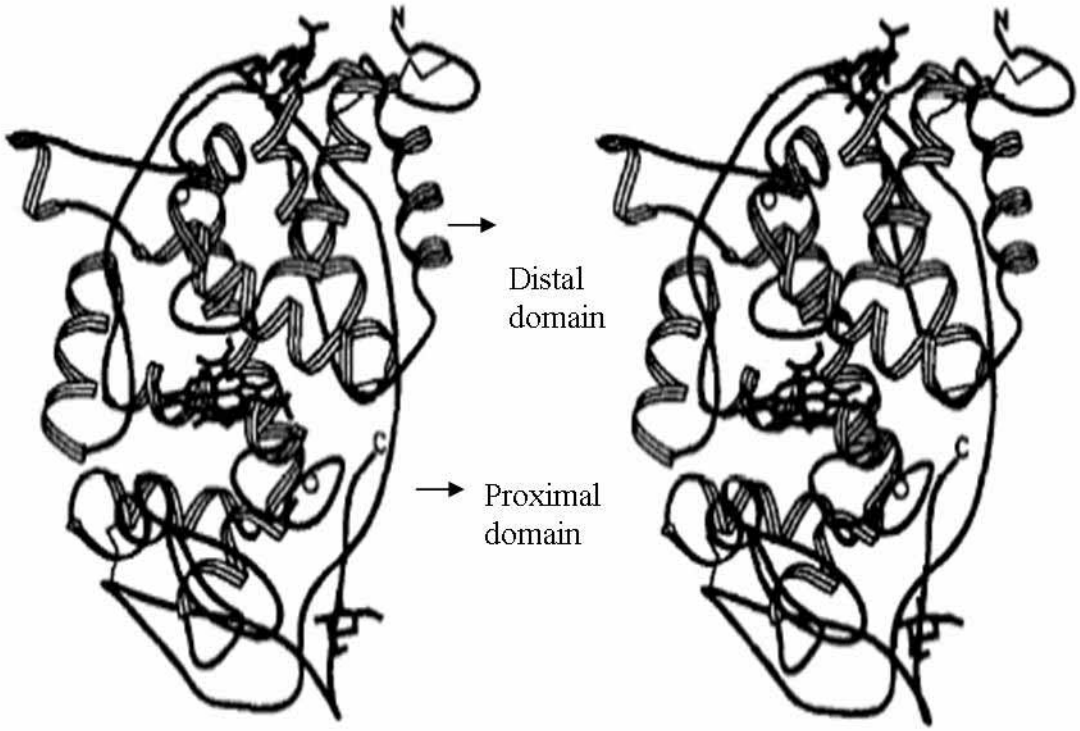

Fig. I-1. The overall fold of the CIP molecule, the heme group, Ca^{2+}ions and bound carbohydrate are also shown (1) .

CIP is a heme-containing enzyme with a heme group coordinates to the N^{ε}-atom of the His184 (*18*). The heme is a porphyrin with an iron atom at the center. The coordination of the heme of CIP is at the penta-coordinated high spin at pH 7.0 and is changed at acidic and alkaline pH (*17*). The absorption peak of porphyrins is at around 400 nm. However, in CIP, the porphyrin exhibits a Soret maximum at 405 nm at neutral pH and at 410 nm at pH 12.1. The extinction coefficient at 405 nm ($\varepsilon_{405\ nm}$) is 109 $mM^{-1}cm^{-1}$and 40 $mM^{-1}cm^{-1}$ for unfolded CIP (*19*).

CIP contains two structurally bound calcium ions that are suggested to maintain the protein structure (*16, 20-23*). One is bound in the proximal and another in the distal domain of CIP (Fig. I-1, (*1*)). The ligands to the Ca^{2+} ion in proximal site are eight oxygen atoms from main and side chains of residues (*1*). The distal Ca^{2+} is heptacoordinated with five ligands from the main and side chain residues (*1*) and two water molecules. EDTA was

shown to be able to chelate two structural Ca^{2+} ions present in secretory plant and fungal peroxidases, resulting in denaturing of enzymes. The denaturation can be reversed by adding calcium ions (*24*).

CIP is a glycoprotein with a glycosylation site at N142 in the sequence of NSS is found. Kjalke and colleagues found a N-linked glycan in CIP at Asn142 (*25*) with a sugar chain, two NAGs, attached to this site. An O-glycosyl moiety was also reported to be linked to Thr331 or Ser338 (*26*).

I-3 Catalytic mechanism

The reactions of CIP in the presence of hydrogen peroxide and phenol proceeds via one-electron transfer mechanism (*27*, *28*). At physiological pH, the resting form of CIP contains a pentacoordinated high-spin heme ferric ion that coordinates with distal His56 and Arg52 through water molecule (Fig. I-2). The distal His56 serves as a catalyst to withdraw a proton from one oxygen atom of the hydrogen peroxide to assist the coordination of –OOH to heme iron and heterolytic cleavage of its O-O linkage. Thus, a compound (I) was generated with a rate constant of k_1 (Fig. I-2, Eq. 1). Compound I is capable of oxidizing a hydrogen donor (AH) to a radical product by one-electron oxidation with a rate constant of k_2 (Eq. 2). Compound I is then converted to compound II, which can further oxidize a second hydrogen donor (AH) to produce another radical product (AH ·). Subsequently, the CIP returns to its resting state with a rate constant k_3 (Eq. 3). However, an inactive form of enzyme, verdohemoprotein, may be formed with excess H_2O_2 (*2-6*).

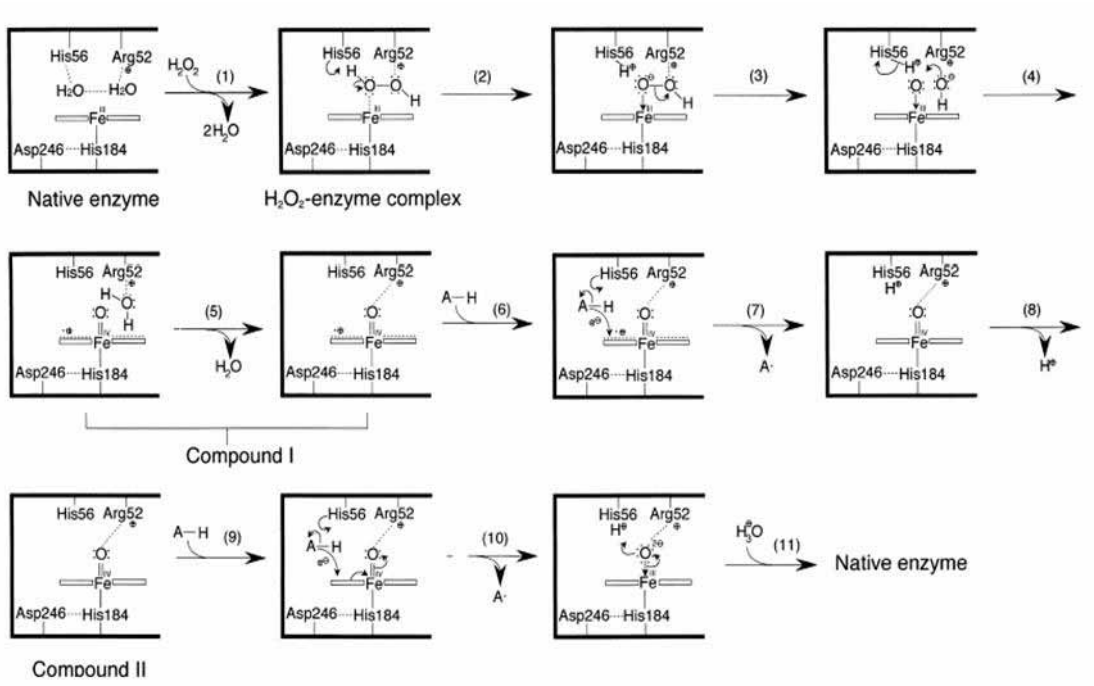

Fig. I-2 Proposed mechanism of ARP or CIP catalysis (2-6).

A conventional peroxidase cycle, and the sum of the three reactions, are as follows:

$$CIP + H_2O_2 \xrightarrow{k_1} Compound\ I + H_2O \text{ (Eq. 1)}$$

$$Compound\ I + AH_2 \xrightarrow{k_2} Compound\ II + \cdot AH \text{ (Eq. 2)}$$

$$Compound\ II + AH_2 \xrightarrow{k_3} CIP + \cdot AH + H_2O \text{ (Eq. 3)}$$

$$H_2O_2 + 2AH_2 \rightarrow 2 \cdot AH + 2H_2O \text{ (Eq. 4)}$$

The velocity of the reaction (v) is expressed as:

$$v = -2d[H_2O_2]/dt = -d[AH_2]/dt \text{ (Eq. 5)}$$

The k_1, the rate of compound I formation, is constant at neutral and alkaline pHs and decreases at acidic pHs with a pK_a of 5.0. The estimated k_1 values at neutral and alkaline pHs are 6–10 × 10^6 $M^{-1}s^{-1}$. The k_2 value shows a bell-shaped pH dependence with a maximum (> 120 × 10^6 $M^{-1}s^{-1}$) at pH 8.0 with pK_a values of 7-9 (*27*). The k_3 value shows a bell-shaped pH dependence with a maximum (48 × 10^6 $M^{-1}s^{-1}$) at pH 8.0 with pK_a values of 7-9 (*27*).

In previous report (*29*), CIP/ARP shows a higher activity to various substrates than

HRP. The V_{max} of CIP/ARP for luminol and 2,4 dichlorophenol are 500 and 2.98 times greater than that of HRP, respectively. The V_{max} value of CIP/ARP for ABTS is also higher than that of HRP. Moreover, CIP/ARP and HRP exhibit similar K_m values to various substrates. Compared with HRP, CIP exhibits a high sensitivity for the determination of hydrogen peroxide.

I-4 Heterologous expression of fungal peroxidase

The heterologous expression of fungal peroxidases have been reported previously (*30*). For example, manganese peroxidase (MnP) isozyme H4 was produced successfully using the baculovirus expression system. PchrMnP (*Phanerochaete chrysosporium* manganese peroxidase;) was successfully produced in different Aspergillus species. Expression of CPO (in *S. cerevisiae*) did not result in any detectable extracellular activity. However, low yield is the main problem that erodes its future application (*30*).

Heterologous expression of *Coprinus cinereus* peroxidase to yield active enzyme has been studied in *S. cerevisiae* and *A. oryzae* (*31, 32*). However, the expression of CIP in *E. coli* has not been explored. Other fungal peroxidases tried to be expressed in *E. coli* were unsuccessful, forming inclusion bodies of apoenzymes (*33*). The production of recombinant CIP in *E. coli* also results in the non-glycosylated enzyme. This apoenzyme is catalytically inactive with the unproper insertion of heme to the recombinant CIP. However, the advantages of using *E. coli* to produce recombinant CIP can be considerable due to the ease of scale-up and the low costs involved in growing bacteria. In addition, protoporphyrin with various metal ions is reconstitued into the apoenzyme.

Many reports showed that the apoenzyme from inclusion body could be refolded upon concentrations of urea, calcium ions, heme and oxidized glutathione (*34, 35*). Before refolding, the inclusion body was solubilized in urea which weakened both hydrogen

bonding and hydrophobic interactions. The urea solubilized inclusion body can be refolded by simply diluting urea. In our work, the optimized conditions for the refolding of CIP was performed by varying the concentrations of urea, DTT, oxidized glutathione, hemin, and calcium.

I-5 Application of peroxidases

Peroxidases have been shown to be used widely in clinical diagnosis enzyme immunoassays, histological chemistry, cancer therapy, and in the development of biosensors. Peroxidase can trigger the conversion of nontoxic indole-3-acetic acid (Auxin) to a toxic product and induce the apoptosis of tumor cells (*36, 37*). Peroxidase can be coupled with oxidase in a bi-enzyme assay system for the determination of various analytes, including biogenic amines, glucose, cholesterol, uric acid and many more metabolites.

Peroxidase have been proven to be superior in the chromogen-based chemiluminescence analysis. Luminescent analysis is 10^2-10^3 times more sensitive than that of the equivalent spectrophotometric method. However, chemiluminescence enhancer needs to be added to the HRP-based chemiluminescent system to increase the efficiency of oxidative degradation of chromogen. Interestingly, CIP or ARP can be used to trigger chemiluminescence reactions in the absence of chemiluminescence enhancer and shown to have higher catalytic efficiency than that of HRP (*29*).

Peroxidases were also shown in the removal of the phenolic wastes in the sewage waste water. The peroxidases from horseradish (HRP), Arthromyces ramosus (ARP) and soybean (SBP) effectively were used frequently to remove the phenolic compounds from solutions (*38-41*).

Although CIP shows higher catalytic activity than HRP, the enzyme is not very stable under thermal conditions. The oxidative stability of *Coprinus cinereus* peroxidase could be

enhanced by substituting single and multiple amino acids near the substrate channel or active centre of the enzyme (*42*). In addition, the stability of CIP was shown to be significantly improved by combining with random mutagenesis and in vivo DAN shuffling (*43*).

I-6 Aims of this study

The recombinant CIP is intended to be expressed in *E. coli* strain BL21(DE3). The expressed recombinant CIP will be characterized by its activity, the kinetics of CIP to various substrates, and its thermal stability.

II. Materials and methods

II-1 Materials

2,2'-azino-bis-3-ethylbenzothiazoline-6-sulfonic acid (ABTS), 4-aminoantipyrine (4-AAP), DMSO, MBTH, DMAB, DTT, and hemin were purchased from Sigma. Glycerol, Na_2HPO_4, NaH_2PO_4, NaOH, KH_2PO_4, and sodium acetate were purchased from SHOWA. Trptone, and yeast extract powder were purchased from USB. Acetone was purchased from C-ECHO. Ammonium sulfate and K_2HPO_4 were purchased from Riedel-de Haen. Urea was purchased from J.T. Baker. Agarose was purchased from gene bank. NaCl, Tris, and glycine were purchased from AMRESCO. EDTA was purchased from Mallinckrodt. SDS-b, acrylamide, and oxidized glutathione were purchased from MD Bio. Bis-tris was purchased from MD biomedical. Acetone was purchased from PANREAC. Ammonium persulfate, and $CaCl_2$ were purchased from YAKURI. Imidazole was purchased from Fluka. Phenol was purchased from biobasic Inc. Bradford reagent was obtained from Bio-Rad. Protein MW marker were purchased from MBI. All restriction enzyme were purchased from the NEB. Taq Dna polymerase and pGEM-T easy vector were purchased from invitrogen.

II-2 Instruments

Instrument	Company
Spectrophotometer	HITACHI U-1100 and HITACHI U-3010, America
Orbital shaking incubator	YIH DER/CM570R
PCR machine	Applied Biosystem/GeneAmp 9700
FPLC system	Amersham Bioscience ÄKTA prime

	plus
SDS-PAGE mini-vertical Gel Electrophoresis	Amersham Bioscience Hoefer SE 260/ Bio-rad
Image System	Pharmacia/ImageMaster®VDS
Thermo-incubator	FIRSTEK/DB102
	FIRSTEK/DB101
Centrifuge	Beckman, Avanti J-E centrifuge
	Eppendorf centrifuge 5415D
	Eppendorf centrifuge 5415R
CD spectropolarizer	Jasco J715
DSC	CSC N-DSC II Model 6100

II-3 Construction of bacterial expression plasmid

To obtain a construct expressing CIP in *E. coli* BL21(DE3) cDNA of the CIP gene (1035 bp) from pET30b(+) (*44-46*) was amplified by polymerase chain reaction (PCR) with the following primer set:

L: 5'-AAGCTTCAGGGTCCTGGAGGAGGCG - 3' (sense)

R:5'-AAGCTTAGGAGCAGGAGCGAGGGAGG -3' (antisense)

The primer pair contains a Hind III restriction site at 5' end. The PCR product was inserted into an pGEM-T easy vector via "cohesive" ends and transformed into *E. coli* strain DH5α. The transformed DH5α clones were plated on a LB/ampicillin/X-gal agar plated and incubated at 37 ℃ for over-night. Selected single colonies were amplified by incubating in 1 mL of LB/ampicillin medium and shaking with 150 rpm at 37 ℃ for 12 h. Plasmid was isolated from 1 mL of *E. coli* cultures by a microprep protocol (GENEAID) as suggested by manufacture. The purified plasmid was checked with its size by digestion with

restriction enzyme Hind III (1035 bp) to check the size and sequence by DNA sequencing to confirm the absence of any mutation. The cleavage of Hind III yields a fragment of 1035 bp containing the cDNA of CIP. This fragment was then inserted into the same sites of the expression vector pET30b(-S), a S-tag removal variant, to give a final plasmid pET30b(-S)-CIP with a length of 6309 bp. This constructed plasmid was checked with restriction enzymes cleavage at Hind III (or EcoRI-XhoI) shown in Fig. 1A. The plasmids were used for the expression of recombinant CIP.

II-4 Expression of *Coprinus cinereus* peroxidase

The expression vector pET30b(-S)-CIP transformed *E.coli* strain BL21(DE3) was first amplified in a 5 mL culturing tube, then transferred to a 500 ml flask containing 250 ml LB medium containing 25 μg/μL kanamycin. The bacterial culture was then shake at 37 ℃ at a speed of 200 rpm. Expression of recombinant CIP was initiated by adding 50 μM IPTG (isopropyl-β-pthiogalactopyranoside) in the mid-log phase of cell growth (0.5-0.7 absorbance unit at 600 nm), followed by cultivation at 37 ℃ and 200 rpm for 10-20 hours. The biomass was collected by centrifugation at 6000 rpm for 20 min at 4 ℃.

II-5 Isolation of inclusion bodies

The bacterial pellet was resuspend in 5 mL of 50 mM Tris-HCl buffer, pH 8.5 containing 10 mM DTT and 2 M NaCl, followed by sonication (on 2 s, off 1 s, 30 %) for 9 min, followed by incubation at 25 ℃ for 1.5 h. Repeat the above process once. The inclusion body were collected by centrifugation at 6000 rpm for 15 min. The inclusion bodies was resuspension in 50 mM Tris-HCl buffer (pH 8.5), and centrifugation at 6000 rpm for 15 min. Repeat the washing two more times. Finally, the inclusion body was resuspended in 50 mM Tris-HCl buffer (pH 8.5) and stored at 4 ℃.

II-6 Renaturation of recombinant CIP

The inclusion bodies of recombinant CIP were completely dissolved in 6 M urea with gentle stirring for 1 hour at 4℃. The final concentration of recombinant CIP was adjusted to 0.5 mg/mL by 6 M urea.

The dissolved CIP apoprotein (0.5 mg/mL) was then added drop-by-drop to the refolding buffer (1.8 M urea, 5 mM calcium chloride, 5 μM hemin and 5 % glycerol in 50 mM Tris-HCl buffer, pH 9.5) in a ratio of 1:10 with gentle stirring. The CIP solution was incubated at 4 ℃ for 8-16 h with a gentle stirring. The refolding medium was optimized by testing with various concentrations of urea (1.5-2.4 M), DTT (0-1 mM), GSSG (0-1 mM), calcium chloride (0-100 mM), hemin (0-20 μM) or KCl (0-100 mM) in fixed 5 % glycerol in 50 mM Tris-HCl buffer at pH 9.5. The enzyme activity of CIP at different stages was measured (as described in section II. 8) to determine the efficiency of renaturation.

II-7 Purification of recombinant CIP

The purification of renatured CIP was performed first by precipitation with 60% ammonium sulfate. The precipitated CIP was collected by centrifugation at 15,000 rpm for 30 min. The pellet was then dissolved in 50 mM Tris-HCl buffer (pH 8.5) and filtered through a 0.45 μm filter to undissolved particulates. The filtrate (< 5 mL) was applied to a Hiprep 16/60 sephacryl S-200 column equilibrated with 50 mM Tris-HCl buffer, pH 8.5 containing 150 mM NaCl with a flow rate of 0.5 ml/min. Eluent was collected on a fraction collector with 4 mL per fraction. Fractions containing CIP were determined by activity assay. Fractions with peroxidase activity were then pooled and concentrated on a Amicon spin column (15 mL) to a volume of 1 mL. To further purify the enzyme, CIP can be applied onto the same column. Active fractions were finally pooled and stored at 4 ℃ or

-20 ℃ in 30% glycerol.

II-8 Peroxidase activity assay

The enzyme activity of recombinant CIP was assayed on a U3010 spectrophotometer. The activity assay was performed by adding 1 μL of 2.86 ng/μL recombinant CIP in 399 μL reaction mixture (100 mM sodium acetate buffer, pH 5.2 with 0.5 mM ABTS (ammonium 2,2'-azino-bis (3-ethylbenzothiazoline-6-sulfonate)) and 5 mM hydrogen peroxide) and incubating at 25 ℃ for 1 min. The extinction coefficient (ε_{ABTS}) of oxidized ABTS at O.D. 405 nm is 36.8 $mM^{-1}cm^{-1}$ (*47*). The enzyme activity of recombinant CIP can also be determined by a colorimetric assay using phenol and 4-AAP as substrates. The activity assay was performed by mixing 1μL of 71.4 ng/μL CIP with 399μL reaction mixture (phenol, 2.4 mM 4-AAP and 0.2 mM H_2O_2 in phosphate buffer pH 7.4) at 25 ℃ for 1 min. The formation of 4-AAP-phenol complex after reaction can be determined at O.D. 510 nm (*48*). The enzyme can also be measured by a colorimetric assay using MBTH and DMAB (MBTH-DMAB, ε = 18.7 $mM^{-1}cm^{-1}$) at 590 nm at 25 ℃ (*49*). The activity assay was performed by mixing 1μL of 221 ng/μL CIP with 399μL reaction mixture (MBTH, 2 mM DMAB, 0.2 mM H_2O_2 in 0.5 M phosphate-citrate buffer, pH 4.0) at 25 ℃ for 1 min.

II-9 Protein concentration determination

Protein concentration was determined by Bradford protein assay (Bio-rad) using bovine serum albumin as a standard. To a 1-mL assay mixture, 1μL protein solution was mixed with 200 μL Bradford reagent and 799 μL d.d. H_2O, at room temperature. The resulting brown-blue mixture was determined at O.D. 595 nm.

II-10 Gel electrophoresis of protein

SDS-PAGE was performed on a Bio-rad Mini protein II apparatus. Proteins (10 μg) was mixed with 5X sample buffer and heated at 95 ℃ for 5 min. The protein sample (10 μg) was loaded onto 10 % SDS polyacryamide gel and subjected to electrophoresis at 70 V for 30 min. The electrophoresis was further performed at 100 volts for another 140 min. After electrophoresis, the gel was stained with stained solution (0.1 % comassie brilliant blue R250, 10 % acetic acid and 50 % methanol) for 1 h, followed by incubating in destaining solution I (10 % acetic acid and 50 % methanol) for 30-60 min. Finally, the gel was incubated in destaining solution II (7 % acetic acid and 5 % methanol) for 2 hours or until background of gel was clear.

II-11 Catalytic properties of recombinant CIP

II. 11.1 Determination of optimal pH and temperature

The enzyme activity was measured at different pH values, such as 2.2, 3, 4, 5, 6, 7, 8, 9 and 10, for enzymes stock (286 ng/μL) in buffer at pH 8. The enzyme was added to an assay buffer in cuvette which was thermostated by means of a circulating bath. The enzyme was treated by varying the temperature from 16℃ to 40℃ (16, 25, 35, and 40 ℃).

The enzyme was incubated at eleven different pH as 2.2, 3, 4, 5, 6, 8, 9 , 10 , 11 and 12 at 25 ℃ for a 7-day period, followed by enzyme activity assay toward ABTS. The buffer were: 0.2 M Gly-HCl at pH 2.2 - 3; 0.2 M sodium acetate at pH 4 - 5; 0.2 M K-phosphate at pH 6 - 8; 0.2 M Tris-HCl at pH 9-10.

II. 11.2 Kinetic parameters of recombinant CIP

The kinetics of recombinant CIP (in the reaction buffer (10 mM phenol, 2.4 mM 4-AAP, 0.1 M phosphate buffer at pH 7.4)) was studied in the presence of various concentration of hydrogen peroxide (0.0125 mM, 0.025 mM, 0.05 mM, 0.1 mM, 0.2 mM,

0.3 mM, 0.4 mM, 0.5 mM, 0.8 mM, 1.2 mM, 1.6 mM, 2.0 mM). The rate of product generation was monitored at O.D. 510 nm and calculated using linear regression on the linear portion of the plot of absorbance vs. reaction time. The rate of hydrogen peroxide consumption in the activity assay is calculated according to single line ($d[H_2O_2]/dt = dA_{510}\varepsilon^{-1}L^{-1}/dt$).

A plot of $[H_2O_2]$ versus activity gives a non-linear curve and fitted on software SIGMA plot based on following equation (Eq. 6) (*50*)

$$R = (\alpha+\beta/ [H_2O_2]+\gamma[H_2O_2])^{-1} \text{ (Eq. 6)}$$

These parameters (α, β, γ) can be substituted into the following equation:

$$a/\alpha = b/\beta = c/\gamma \text{ (Eq. 7)}$$

where a (model parameter, s) and α (model parameter, dimensionless) control the rates of aromatic substrate utilization, b (model parameter, $molL^{-1}s$) and β (model parameter, $molL^{-1}$) control the rates of hydrogen peroxide utilization, and c (model parameter, $mol^{-1}L$ s) and γ (model parameter, $mol^{-1}L$) control the rates of inhibition through compound III formation.

$$a = KC_a/(1+\beta/ \alpha / [H_2O_2]_s+\gamma[H_2O_2]_s/\alpha \text{)(Eq. 8)}$$

where K is a proportional constant ($A_s = -K\times d [H_2O_2]/dt$; As, Activity measured at the standard hydrogen peroxide concentration (UL^{-1})), C_a is the proportionality constant relating the molar concentration of peroxidase to the corresponding activity (i.e., $C_a = E_o/A_s$), $[H_2O_2]_s$ is the standard concentration of H_2O_2 (2×10^{-4}M). The values of a, b, and c can be obtained, and then the values of k_1 and $(1/k_2 + 1/k_3)^{-1}$ can be calculated individually from the following equation:

$$a = 1/2[PhOH]_s(1/k_2 + 1/k_3) \text{ (Eq. 9)}$$

$$b = 1/2k_1 \text{ (Eq. 10)}$$

Where k_1 is the rate constant of peroxidase to take H_2O_2; k_2 and k_3 are the rate constants of

the one-electron oxidation of Compound I and Compound II, respectively (Fig. II-1).

The hydrogen peroxide concentration that results in maximum peroxidase activity $[H_2O_2]_{maxR}$ can be calculated as:

$$[H_2O_2]_{maxR} = (\beta/\gamma)^{1/2} = (b/c)^{1/2} \text{ (Eq. 11)}$$

In addition, the parameters were also determined by Lineweaver-Burk plot, as shown below:

$$1/V = K_m/V_{max} \times 1/[S] + 1/V_{max} \text{ (Eq. 12)}$$

The curve fitting was performed using SIGMA plot (*50*).

II-12 Spectrophotometric studies of the stability of recombinant CIP

The recombinant CIP (63.2 U in 10 μL) was incubated first in 50 mM Tris-HCl buffer, pH 8.0 at 25 ℃, 35 ℃, 55 ℃ and 80 ℃ for 5 - 20 min. After incubation, recombinant CIP was then assay for the remainant enzyme activity. The effect of Ca^{2+} ion on the heat-denaturation/reactivation of CIP was also studied. CIP (63.2 U) was treated at 55 ℃ for 5 min in the presence of mock, 1 mM EDTA, or 1 mM EDTA and then add 1 mM $CaCl_2$ at 4 ℃ for 20 min. The enzyme activity of treated CIP was then measured for its remainant enzyme activity. The time-dependent absorption of recombinant CIP at O.D. 404 nm upon thermal treatment/reactivation was also determined on U3010 spectrophotometer (Hitachi).

The 1 mL protein solution (63.2 U CIP) was placed in a cuvette that was thermostated in the chamber of Hitachi U3010 spectrophotometer with a circulating water bath. The heat-denaturation of CIP was directly monitored at 404. The stability of recombinant CIP

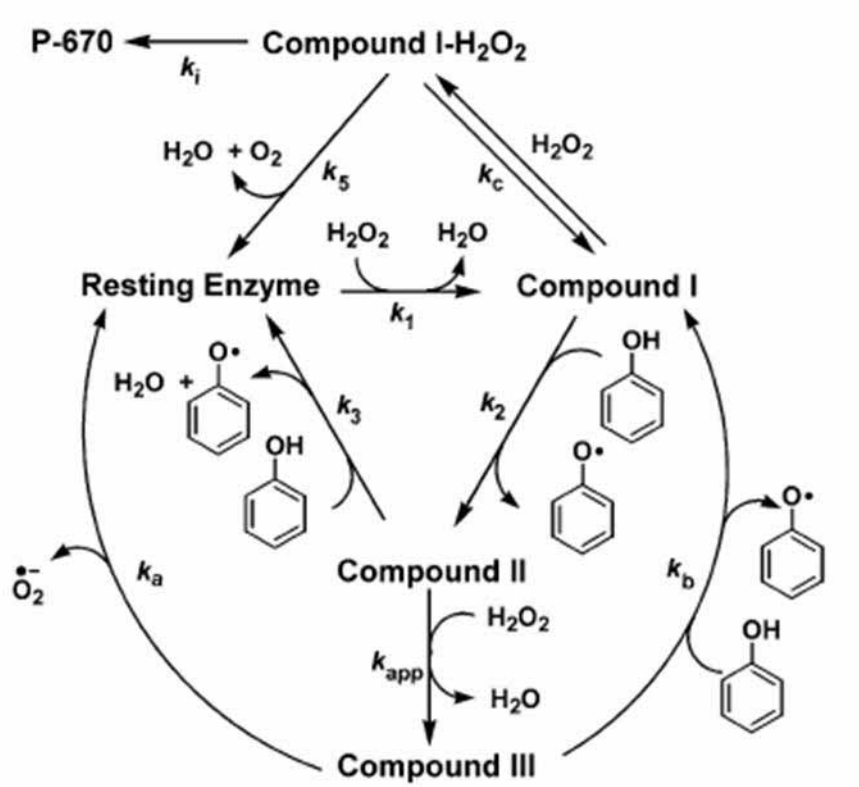

Fig. II-1. Catalytic cycle of peroxidase. P-670 is a permanently inactivated form of enzyme called verodohaemoprotein (Ikehata et al., 2005).

was analyzed based on the method proposed by Tams and Welinder (*51*). Accordingly, a plot of ΔA versus time (s) was generated.

$$\Delta A = (A_t - A_\infty)/(A_0 - A_\infty) \quad \text{(Eq. 13)}$$

Where, A_t is the absorbance at time t during heat denaturation; A_0 is the absorbance at the beginning of the experiment; A_∞ is the absorbance of protein solution at the end of the heat denaturation. The experimental curve was fitted using SIGMA plot based on first-order expression as presented in Eq.14 (monophasic reaction) and Eq. 15 (for biphasic reaction):

$$\Delta A = \exp(-t/\tau) \text{ (monophasic reaction)} \quad \text{(Eq. 14)}$$

$$\Delta A = P1\exp(-t/\tau 1) + P2\exp(-t/\tau 2) \text{ (biphasic reaction)} \quad \text{(Eq. 15)}$$

where τ 1 and τ 2 are time constants for unfolding. The time constant exhibits an inverse

relationship with the rate constants of unfolding k_u and folding k_f .

$$\tau = 1/(k_u+k_f) \text{ (Eq. 16)}$$

When folding of protein is arrested (EDTA) , $k_f = 0$, then

$$\tau = 1/(k_u) \text{ (Eq. 17)}$$

The activation free energy ($\Delta G^{\neq}_u$) can be calculated according the Eyring assumption:

$$\Delta G^{\neq}_u = -RT\ln(k_u h)/(k_b T) \text{ (Eq. 18)}$$

Where, h is a plank constant, 6.626×10^{-34} J s; k_b is a Boltzmann constant, $1.3806505 \times 10^{-23}$ J/K, R is universal constant, 8.3145 J/mol, T is absolute temperature (K) (*51*).

II-13 Thermodynamic properties of CIP

The effect of 4 mM EDTA on the heat denaturation of CIP could be monitored at 404 nm on U3010 spectrophotometer. The rate constants were derived from the major phase of the biphasic reactions or monophasic reactions (Eq. 14 and Eq. 15). A plot of $\ln k_u$ versus 1/T (in Kelvins) would yield a slope of $-E_a/R$. Where, E_a is the activation energy for denaturation; R is the molar gas constant.

$$\ln k_u = \ln A - E_a/RT \text{ (Eq. 19)}$$

where A is the frequency factor.

As the activation enthalpy $\Delta H^{\neq}_u$ E_a, the contribution from the activation entropy could be calculated from the Eq.10:

$$T\Delta S^{\neq}_u = \Delta H^{\neq}_u - \Delta G^{\neq}_u \text{ (Eq. 20)}$$

II-14 Scanning calorimetry

Heat capacity measurements was carried out on a CSC Nano II Differential Scanning Calorimeter (N-DSC II, Model 6100). Exhaustive cleaning of cells was performed before each experiment. The enzyme solution was dialyzed against 50 mM Tris-HCl, pH 8.5, and

the dialyzate was used as reference. The scan rate 1 K/min was employed. An over-pressure of 3 atm was kept over the liquid in the cells throughout the scans. The heat capacity C_p was measured as a function of temperature between 25 ℃ and 80 ℃. The area under the DSC curve corresponds to the molar enthalpy change ΔH_{cal} for the phase transition. The phase transition temperature (T_m), or called melting temperature, for recombinant CIP was obtained from DSC curves.

II-15 Circular dichroism (CD)

CD experiments were carried out using a Jasco J715 spectropolarimeter. CD in the UV region (190-260 nm) was monitored with a cell of 1 mm path length. CD spectra reported in this study were an average of sixteen scans recorded at a speed of 200 nm/min and a resolution of 1 nm, corrected by subtracting the appropriated blank runs on recombinant CIP free solutions. The percentages of secondary structure elements was calculated using SELCON3 software.

III. Results and discussion

III-1 Expression of recombinat *Coprinus cinereus* peroxidase

The recombinant CIP was expressed in *E. coli* BL21(DE3) by inducing bacterial culture ($O.D._{600\,nm}$ = 0.8) with 0 or 50 μM IPTG at 37 ℃ for 10 or 20 h. After induction, bacteria were collected, lysed with sonication and assayed for the presence of recombinant and the peroxidase activity. The electrophoresis of E. coli inclusion body after 50 μM IPTG induction is shown in Fig. 2A. Inclusion body formation in recombinant *E. coli* cells overexpressing CIP. The peroxidase activity from refolding of inclusion body was also tested. However, the bacterial extracts after 10 or 20 h IPTG induction were not much different between each other. The activity of recombinant CIP in *E. coli* appeared without the induction of IPTG and cannot be enhanced dramatically by increasing concentration of IPTG. It could be due to the constitutive expression of exogenous in *E. coli* BL21 (DE3). This result suggests a deficiency in the suppression of recombinant protein expression in their system.

III-2 Refolding of inclusion bodies

The inclusion bodies was first solubilizd in 6 M urea to make a concentration of 0.5 mg/mL. The solubilized CIP was then subjected to renaturation by diluting in a refolding buffer (1.8 M urea in 50 mM Tris-HCl buffer, pH 9.5 containing 5 mM $CaCl_2$, 5 μM hemin, 0.1 mM DTT, 0.5 mM oxidized glutathione and 5 % glycerol) in a ratio of 1:9 at 4 ℃ for a period of time (0-8 h). The peroxidase activity of the renatured CIP was monitored by transferring 1 μL aliquote of folding mixture to a reaction mixture (399 μL) for enzyme activity assay. As shown in Fig. 3, the recombinant CIP renatured in a time-dependent manner with a maximum reactivation occurred at about 7 h.

The effect of DTT, GSSG, urea, KCl, calcium ion and hemin in the refolding of CIP

was investigated. CIP contains four intramolecular disulfide bonds, which may be perturbed by DTT. DTT also prevents the proteins from unwanted oxidation. However, the renaturation of CIP was significantly perturbed by DTT (Fig. 4A). The refolding of CIP was rapidly suppressed by DTT. GSSG is required for the renaturation of manganese peroxidase (MnP) and tobacco anionic peroxidase (TOP) (*24*, *52*). However, in HRP, the increase concentrations of DTT and GSSG results in decrease of its enzymic activity. Interestingly, GSSG was also found to suppress the renaturation of recombinant CIP (Fig. 4B). The activity of CIP in refolding mixture decreases with increasing concentrations of GSSG from 0.1 to 1.0 mM. The effect of urea concentration in the renaturation of recombinant CIP was also tested. The highest enzyme activity could be observed in the refolding buffer containing 1.8 M urea (Fig. 4C). The urea concentration in renaturation buffer below or above 1.8 M may affect the refolding process, resulting in low enzyme reactivation. Ionic strength, as indicated by KCl concentration (0-100 mM), had no or little effect on the reanturation of CIP (Fig. 4D). The renaturation of the recombinant CIP requires hemin and Ca^{2+} ion. Maximal activity after renaturation occurred when renaturation buffer containing 5 μM hemin (Fig. 4F) or 10 mM $CaCl_2$ (Fig. 4E). The concentration of Ca^{2+} ion higher than 10 mM exhibited less effect in the renaturation of recombinant CIP. The yield of active CIP during renaturation was more sensitive to the hemin concentration. The activity of renatured CIP quickly decreased with hemin higher than 5 μM (Fig. 4F). It is possible that the hydrophobic property of hemin molecule may interfere with the proper folding of CIP. Temperature also affect the renaturation of CIP. The renaturation of CIP at 25 ℃ or 35 ℃ exhibited a much lower renaturation (*53*). Hemin is added after refolding to the apoenzyme restores the enzyme activity of recombinant CIP (Fig. 6). A similar result was also observed in HRP (*54*). However, in the case of tobacco anionic peroxidase, hemin should be added during the refolding (*34*).

III-3 Purification of recombinant CIP

The renatured recombinant CIP was purified from impurities come with inclusion body by first precipitates with 60 % ammonium sulfate followed by sizing exclusion column. The precipitation of recombinant CIP with ammonium sulfate helps to concentrate the enzyme and partly remove impurities. The 60 % ammonium sulfate precipitate may help refolding of recombinant CIP. A marked increase in the specific activity of CIP could be observed (Table 2). In the case of the MnP, the removal of 2 M urea after renaturation by dialysis also increases the specific activity of renatured MnP (*55*). In contrast, a significant activity lost was observed in recombinant tobacco anionic peroxidase precipitating with ammonium sulfate (*52*). The precipitated protein was then further purified on sizing exclusion column. The elution profile of recombinant CIP showed that most protein was eluted in fraction 9 (60-64 ml), where the maximal peroxidase activity appeared (Fig. 7-1). The absorption spectra of several fractions including f1, f3, f5, f7, f9 and f11, between 700 nm and 350 nm. The fractions with higher specific activity exhibited a Soret band at 404 nm. While the recombinant CIP in fractions 3, 5 and 7, presumably have higher molecular weight than that in fraction 9, had a Soret band in a range of 410 ～ 408 nm. This result is consistent with observation that the aggregated TOP exhibits a Soret band at 409 nm. The aggregated CIP in fractions 3-7 also exhibited a low specific activity. The fractions 8-10 were collected and concentrated on Amicon Ultra-4 (centrifugal filter devices). The concentrated CIP was then reloaded on second sizing exclusion column S-200 (Amersham Biosciences, HiPrep 16/60) for further purification. The eluant was collected with 2 or 4 mL per fraction (Fig. 8-1). The high CIP activity appeared in fractions 9 and 10 (Fig. 8-1). The absorption spectra of fractions 2-11 from S-200 column was also scanned between 700 nm and 300 nm (Fig. 8-2). The fractions (9 and 10) with higher activity had Soret band at 404 nm. The RZ (Reinheitszahl) values, as determined by the ratio of A404 nm (λ_{Max} of

Soret band) /A280 nm of isolated CIP in ammonium sulfate precipitation, first gel filtration column and second gel filtration column was 1.7, 2.9 and 3.3, respectively (Table 2). The increasing RZ values along with the purification process suggests the increasing purity of the purified CIP. SDS-PAGE analysis was also performed to evaluate the purity of the purified CIP (Fig 10). Table 2 summarizes the parameters regarding to recombinant CIP during purification. After ammonium sulfate precipitation, the specific activity of the recombinant CIP increased about 5-fold. The removal of urea after precipitation may be the cause of activity increase. A similar result was also observed in MnP (*55*). The specific activity of MnP increases as 2 M urea is removed through dialysis. The reactivation of recombinant CIP was greatly affected by DTT and GSSG (Fig. 4A and 4B). However, once DTT and GSSG were removed after ammonium sulfate precipitation, the recombinant CIP exhibited similar specific activity to that without DTT and GSSG during reactivation. Although DTT and GSSG may inhibit the activity of recombinant CIP during reactivation, they may not affect the refolding of recombinant CIP (Table 1).

III-4 The optimal condition for reaction of CIP

Previously, CIP was reported to react optimally at 40 ℃, and a pH range from 5.0-9.0 depending on substrate used (*13, 29, 56*). To investigate the optimal condition for recombinant CIP, its enzymatic activity was assayed at different pH values (pH 2.2-10). The recombinant CIP exhibit a maximum activity at pH 5 (Fig. 11) and 35 ℃ (Fig. 12) by using ABTS as substrate.

III-5 Kinetics study of recombinant CIP

The kinetics of recombinant CIP to H_2O_2 and phenolic substrates such as phenol and MBTH was investigated. The oxidation of phenol (0.5-40 mM) by H_2O_2 was catalyzed by

recombinant CIP (Fig. 13-1). Fig. 13-2 shows a plot of 1/ [phenol] vs 1/ V that yields a K_m of 8.3 mM with a V_{max} of 5.76×10^2 μmol/min/mg. The data of Fig. 13-2 was fitted to the equation, $1/V = K_m/V_{max}\ 1/S + 1/V_{max}$. The kinetic parameters of recombinant CIP for phenol and MBTH are summarized in Table 4 (data of Fig.13-1 to 16-2). The K_m (AH_2) values of recombinant CIP for phenol and MBTH were 8.3 mM, and 0.005 mM, suggesting a higher affinity for MBTH than that of phenol. The K_m values of recombinant CIP for H_2O_2 were 0.87 mM or 0.90 mM by using phenol and MBTH as substrates, respectively. The V_{max} for phenol and MBTH was 5.39×10^3 μmol/min/mg by using phenol as substrate and 6.19×10^2 μmol/min/mg by using MBTH as substrate (Table 4). The K_{cat}/K_m, a representative of catalytic efficiency, was 2.53×10^5 $mM^{-1}min^{-1}$ for phenol and 2.82×10^4 $mM^{-1}min^{-1}$ for MBTH (Table 4), respectively.

III-6 Effect of calcium and EDTA on the thermal stability of recombinant CIP

The thermal stability of CIP was studied under temperatures from 25 ℃ to 80 ℃. At 25 ℃ and 35 ℃, recombinant CIP is stable for at least 20 min (Fig. 17). However, when treating recombinant CIP at temperature above 55 ℃, a dramatic decrease in activity occurred within 5 min (Fig. 17). EDTA or EGTA are chelating agents that take up calcium ions from peroxidases and may cause denaturation and inactivation of the recombinant CIP. The stability of recombinant CIP was more sensitive to thermal treatment than that of control in the presence of Ca^{2+} or EDTA (Fig. 18). In the presence of 1 mM EDTA or Ca^{2+}, recombinant CIP was completely inactivated at 55 ℃ in about 5 min (Fig. 18). In contrast, about 40 % recombinant CIP activity remained without Ca^{2+} or EDTA. Excess Ca^{2+} ions has been shown previously to reduce the activity of tobacco anionic peroxidase (TOP) (*52*). The suppressive effect of Ca^{2+} ion to recombinant CIP was also demonstrated here (Fig. 18) . A structural change in CIP due to the adsorption of Ca^{2+} ions on protein surface. The

thermal-induced structural alternation in recombinant CIP was also studied with UV/VIS absorption spectra. Absorption spectrum of native recombinant CIP without heat-treatment at 55 ℃ was performed from 350 nm to 450 nm , generating an absorption band at 404 nm. After treatment at 55 ℃ for 5 min, a significant red shift in the absorption peak from 404 nm to 414 nm occurred for recombinant CIP in the presence of 1 mM EDTA , suggesting a conformational change. The EDTA-dependent, thermal-induced red shift in the absorption peak was reversed by adding Ca^{2+} ions (Fig. 19). The thermally induced conformational change leads to inactivation of recombinant CIP. This thermal inaction of CIP was greatly enhanced by EDTA consistent with previous observation in Fig. 20, thermally inactivated CIP could be reactivated by 1 mM Ca^{2+} (Fig. 21). Calcium ion is required to maintain the protein structure as determined by NMR and metal ion substitution (*23*). In MnP, the thermal inactivation induces the release of distal Ca^{2+} ion from enzyme, resulting in mis-coordination of His46 to the heme iron (*57*). These observation may explain the effect of EDTA in the heat-induced in activation of recombinant CIP.

III-7 Calorimetric experiments

The thermodynamic properties of recombinant CIP were studied by calorimetric study on DSC (differential scanning calorimetry). The thermal denaturation of recombinant CIP at pH 8.5 exhibited a single phase calorimetric transition at a temperature (T_m) of 48 ℃ (Fig. 22). The enthalpy (ΔH) and entropy (ΔS) of the recombinant CIP in thermal denaturation were also calculated as ΔH_{cal} = 348.3 KJ/mol and ΔS = 1.09 KJ/mol/K (Table 5). T_m values can be used to evaluate the stability of enzyme, as the T_m of recombinant CIP is lower than those of other peroxidases, such as T_m = 71.4 ℃ for HRP (*58, 59*), T_m = 86 ℃ for SBP (*60*) and T_m = 74.6 ℃ for AOPTP (*61*) (Table 6). The result indicates that the recombinant CIP prepared in this study is less stable than peroxidases reported previously.

III-8 Thermal induction of CIP conformational changes

Circular dichroism (CD) is one of powerful biophysical techniques for determining secondary structures and monitoring structural changes of biomacromolecules such as proteins and DNA. Recombinant CIP was treated at either 55 ℃ or 80 ℃ for 10 min prior to monitoring on a CD spectropolarimeter (Jasco J715). The far-UV CD spectra of untreated (solid line), or heat-treated at 55 ℃ (dotted lines) or 80 ℃ (dashed line) recombinant CIP at pH 8.5 in 50 mM Tris-HCl buffer is shown in Fig. 23. The spectra is used to estimate the secondary structures, such as α helix, β sheet and β-turn, in recombinant CIP. Recombinant CIP exhibited a peak at 224 nm, which is a indicative of α-helix. When raising the temperature from room temperature to 55℃ or 80℃, the 224 nm absorption peak decreased. The fractions of α-helix, β-strand, turns, and disordered secondary structures were calculated by using accompanied software SELCON3 (Table 7). Heat denaturation at 80 ℃ significantly altered the secondary structure of recombinant CIP exhibiting an increase in disordered structure from 24.9 %, for untreated recombinant CIP, to 35.4 % for heat-treated one at 80 ℃. The level of α-helices in recombinant CIP also decreased from 46.5 % to 15.5 % after thermal denaturation at 80℃.

III-9 Stability of recombinant CIP under different pH values

The effect of pH in the stability of recombinant CIP was investigated by incubating the enzyme in buffers with different pH values at 25 ℃ for 7-day (Fig. 24). At pH values below 4 and above 11, the enzyme activity lost quickly within 1 day. However, within the range of pH 5 and pH 9, the enzyme activity of CIP declined to about 60 % in 1 day and remained at this activity level for at least 6 days. However, native CIP was shown previously to maintain its 100 % activity within pH range 5 to 9 in 5 days (*39*).

III-10 Steady state UV/VIS absorption spectra of recombinant CIP

The absorption and resonance Raman spectra of native CIP exhibits a 5-cooridinated high spin (5cHS) with Soret band at 403 nm, α band at 534 nm, β band at 505 nm and a charge transfer band (CT1, from porphyrin to the heme iron) at 649 nm (*17*). At pH 11.6, the absorption of CIP spectra exhibits peaks at 404, 505, 530, 570 and 645 nm (11). The weak band at 570 nm , the α band of 6-coordinating low spin (6cLS) indicates the existence of a small fraction of 6cLS heme. In case of recombinant CIP, the absorption spectra maxima could be observed at 404 nm (Soret band), 504 nm (β band) and 641 nm (CT1) nm (Fig. 25). The comparison of the absorption maxima of recombinant CIP and native CIP was shown in Table 8.

IV Conclusion

Refolding of bacterial expressed recombinant CIP is successfully performed in this study. The apoenzyme of CIP can be refolded in the presence of $CaCl_2$, hemin and urea at 4 ℃. Both $CaCl_2$ and hemin are required for the refolding of recombinant CIP. Subsequently, recombinant CIP is purified sequentially through precipitation with 60 % ammonium sulfate and gel filtration column. The yield of recombinant CIP is 15 % with a specific activity of 23544 U/mg.

The thermal stability of recombinant CIP is affected by by Ca^{2+} ion. When incubated with EDTA, the activity of CIP rapidly decreased by heating at 55 ℃. This heat denaturation can be partially rescued by addition of Ca^{2+}.

V References

1. Petersen, J. F., Kadziola, A., and Larsen, S. (1994) Three-dimensional structure of a recombinant peroxidase from *Coprinus cinereus* at 2.6 Å resolution, *FEBS Lett. 339*, 291-296.
2. Nakayama, T., and Amachi, T. (1999) Fungal peroxidase: its structure, function, and application, *J. Mol. Catal. B: Enzym. 6*, 185-198.
3. Farhangrazi, Z. S., Copeland, B. R., Nakayama T., Amachi T., Yamazaki I, and Powers L. S. (1994) Oxidation-reduction properties of compounds I and II of *Arthromyces ramosus* peroxidase, *Biochem. 33*, 5647-5652.
4. Hashimoto, S., Tatsuno, Y., and Kitagawa, T. (1986) Resonance Raman evidence for oxygen exchange between the FeIV = O heme and bulk water during enzymic catalysis of horseradish peroxidase and its relation with the heme-linked ionization, *Proc. Natl. Acad. Sc. USA 83*, 2417-2421.
5. Nagano, S., Tanaka, M., Ishimori, K., Watanabe, Y., and Morishima, I. (1996) Catalytic roles of the distal site asparagine-histidine couple in peroxidases, *Biochem. 35*, 14251-14258.
6. Sitter, A. J., Reczek, C. M., and Terner, J. (1985) Heme-linked ionization of horseradish peroxidase compound II monitored by the resonance Raman Fe(IV)=O stretching vibration, *J. Biol. Chem. 260*, 7515-7522.
7. Smith, A. T., and Veitch, N. C. (1998) Substrate binding and catalysis in heme peroxidases, *Curr. Opin. Chem. Biol. 2*, 269-278.
8. O'Brien, P. J. (2000) Peroxidases, *Chemi. Biol. Interact. 129*, 113-139.
9. Welinder, K. G. (1992) Superfamily of plant, fungal and bacterial peroxidases, *Curr. Opin. Chem. Biol. 2*, 388-393.
10. Kjalke, M., Andersen, M. B., Schneider, P., Christensen, B., Schulein, M., and Welinder, K. G. (1992) Comparison of structure and activities of peroxidases from *Coprinus cinereus*, *Coprinus macrorhizus* and *Arthromyces ramosus*, *Biochim. Biophys. Acta 1120*, 248-256.
11. Petersen, J. F., Tams, J. W., Vind, J., Svensson, A., Dalboge, H., Welinder, K. G., and Larsen, S. (1993) Crystallization and X-ray diffraction analysis of recombinant *Coprinus cinereus* peroxidase, *J. Mol. Biol. 232*, 989-991.
12. Kunishima, N., Fukuyama, K., Wakabayashi, S., Sumida, M., Takaya, M., Shibano, Y., Amachi, T., and Matsubara, H. (1993) Crystallization and preliminary X-ray diffraction studies of peroxidase from a fungus *Arthromyces ramosus*, *Proteins 15*, 216-220.
13. Kunishima N., Fukuyama, K., Matsubara, H., Hatanaka, H., Shibano, Y., and Amachi, T. (1994) Crystal structure of the fungal peroxidase from *Arthromyces ramosus* at 1.9 Å resolution. Structural comparisons with the lignin and cytochrome c peroxidases., *J. Mol. Biol. 235*, 331-344.
14. Kunishima, N., Amada, F., Fukuyama, K., Kawamoto, M., Matsunaga, T., and Matsubara, H. (1996) Pentacoordination of the heme iron of *Arthromyces ramosus* peroxidase shown by a 1.8 Å resolution crystallographic study at pH 4.5, *FEBS Lett. 378*, 291-294.
15. Finzel, B. C., Poulos, T. L., and Kraut, J. (1984) Crystal structure of yeast cytochrome c peroxidase refined at 1.7-Å resolution, *J. Biol. Chem. 259*, 13027-13036.
16. Poulos, T. L., Edwards, S. L., Wariishi, H., and Gold, M. H. (1993) Crystallographic refinement of lignin peroxidase at 2 Å, *J. Biol. Chem. 268*, 4429-4440.
17. Smulevich, G., Neri, F., Marzocchi, M. P., and Welinder, K. G. (1996) Versatility of

heme coordination demonstrated in a fungal peroxidase. Absorption and resonance Raman studies of *Coprinus cinereus* peroxidase and the Asp245-->Asn mutant at various pH values, *Biochem. 35*, 10576-10585.

18. Di Cerbo, P., Welinder, K. G., and Schiodt, C. B. (2001) Kinetic evidence for surface residues influencing the active site of *Coprinus cinereus* peroxidase: analysis of the pH dependence of G154E, P90H and P90H-G154E substrate entrance mutants, *Biochim. Biophys. Acta 1544*, 18-27.
19. Andersen, M. B., Hsuanyu, Y., Welinder, K. G., Schneider, P., and Dunford, H. B. (1991a) kinetics and equilibria of cyanide binding to *Coprinus cinereus* peroxidase, *Acta chemica. Scand. 45*, 206-211.
20. Sutherland, G. R. J., and Aust, S. D. (1996) The effects of calcium on the thermal stability and activity of manganese peroxidase, *Biochem. Biophys. 332*, 128-134.
21. Booth, K. S., Kimura, S., Lee, H. C., Ikeda-Saito, M., and Caughey, W. S. (1989) Bovine myeloperoxidase and lactoperoxidase each contain a high affinity site for calcium, *Biochem. Biophys. Res. Commun. 160*, 897-902.
22. Haschke, R. H., and Friedhoff, J. M. (1978) Calcium-related properties of horseradish peroxidase, *Biochem. Biophys. Res. Commun. 80*, 1039-1042.
23. Shiro, Y., Kurono, M., and Morishima, I. (1986) Presence of endogenous calcium ion and its functional and structural regulation in horseradish peroxidase, *J. Biol. Chem. 261*, 9382-9390.
24. Reading, N. S., and Aust, S. D. (2000) Engineering a disulfide bond in recombinant manganese peroxidase results in increased thermostability, *Biotechnol. Prog. 16*, 326-333.
25. Kjalke, M., Andersen, M. B., Schneider, P., Christensen, B., Schulein, M., and Welinder, K. G. (1992) Comparison of structure and activities of peroxidases from *Coprinus cinereus*, *Coprinus macrorhizus* and *Arthromyces ramosus*, *Biochim. Biophys. Acta. 1120*, 248-256.
26. Baunsgaard, L., Dalboge, H., Houen, G., Rasmussen, E. M., and Welinder, K. G. (1993) Amino acid sequence of *Coprinus macrorhizus* peroxidase and cDNA sequence encoding *Coprinus cinereus* peroxidase. A new family of fungal peroxidases, *Eur. J. Biochem. 213*, 605-611.
27. Abelskov, A. K., Smith, A. T., Rasmussen, C. B., Dunford, H. B., and Welinder, K. G. (1997) pH Dependence and Structural Interpretation of the Reactions of *Coprinus cinereus* Peroxidase with Hydrogen Peroxide, Ferulic Acid, and 2,2'-Azinobis (3-ethylbenzthiazoline-6-sulfonic acid), *J. Clin. Chem. Clin. Biochem.* 17, 9453-9463.
28. Farhangrazi, Z. S., Copeland, B. R., Nakayama, T., Amachi, T., Yamazaki, I., and Powers, L. S. (1994) Oxidation-Reduction Properties of Compounds I and II of *Arthromyces ramosus* Peroxidase, *Biochem. (Mosc). 33*, 5647-5652.
29. Akimoto K., Shinmen, Y., Sumida, M., Asami, S., Amachi, T., Yoshizumi, H., Saeki, Y, Shimizu, S., and Yamada, H. (1990) Luminol chemiluminescence reaction catalyzed by a microbial peroxidase, *Anal. Biochem. 189*, 182-185.
30. Conesa, A., Punt, P. J., and van den Hondel, C. A. M. J .J. (2002) Fungal peroxidases: molecular aspects and applications, *J. Biotechnol. 93* 143–158.
31. Andersen, H. D., Jensen, E. B., and Welinder, K. G. (1992) A process for producing heme proteins., *European Patent Application no.0505311A2.*
32. Sawai-Hatanaka, H., Ashikari, T., Tanaka, Y., Asada, Y., Nakayama, T., Minakata, H., Kunishima, N., Fukuyama, K., Yamada, H., and Shibano, Y. (1995) Cloning, sequencing, and heterologous expression of a gene coding for *Arthromyces ramosus* peroxidase., *Biosci. Biotechnol. Biochem. 59*, 1221-1228.

33. Doyle, W. A., and Smith, A. T. (1996) Expression of lignin peroxidase H8 in Escherichia coli: folding and activation of the recombinant enzyme with Ca^{2+} and haem, *Biochem. J. 315*, 15-19.
34. Hushpulian, D. M., Savitski, P. A., Rojkova, A. M., Chubar, T. A., Fechina, V. A., Sakharov, I. Y., Lagrimini, L. M., Tishkov, V. I., and Gazaryan, I. G. (2003) Expression and refolding of tobacco anionic peroxidase from E. coli inclusion bodies, *Biochem. (Mosc) 68*, 1189-1194.
35. Smith, A. T., Santama, N., Dacey, S., Edwards, M., Bray, R. C., Thorneley, R. N., and Burke, J. F. (1990) Expression of a synthetic gene for horseradish peroxidase C in *Escherichia coli* and folding and activation of the recombinant enzyme with Ca^{2+} and heme, *J. Biol. Chem. 265*, 13335-13343.
36. Bagshawe, K. D., Sharma, S. K., and Begent, R. H. (2004) Antibody-directed enzyme prodrug therapy (ADEPT) for cancer, *Expert Opin. Biol. Therapy 4*, 1777-1789.
37. Senter, P. D., and Springer, C. J. (2001) Selective activation of anticancer prodrugs by monoclonal antibody-enzyme conjugates, *Adv. drug del. rev. 53*, 247-264.
38. Ikehata, K., and Buchanan, I. D. (2002) Screening of Coprinus species for the production of extracellular peroxidase and evaluation of the enzyme for the treatment of aqueous phenol, *Enviro. Techno. 23*, 1355-1367.
39. Ikehata, K., Buchanan, I. D., Pickard, M. A., and Smith, D. W. (2005) Purification, characterization and evaluation of extracellular peroxidase from two Coprinus species for aqueous phenol treatment, *Bioresour. Technol. 96*, 1758-1770.
40. Ikehata, K., Buchanan, I. D., and Smith, D. W. (2004) Extracellular peroxidase production by Coprinus species from urea-treated soil, *Canad. J. Microbio. 50*, 57-60.
41. Ikehata, K., Pickard, M. A., Buchanan, I. D., and Smith, D. W. (2004) Optimization of extracellular fungal peroxidase production by 2 Coprinus species, *Canad. J. Microbio. 50*, 1033-1040.
42. Welinder, K. G. (1993) Peroxidase variants with improved hydrogen peroxide stability., *Internation patent application WO 93/24618*.
43. Cherry, J. R., Lamsa, M. H., Schneider, P., Vind, J., Svendsen, A., Jones, A., and Pedersen, A. H. (1999) Directed evolution of a fungal peroxidase., *Nat. Biotechnol. 17*, 379-384.
44. 何威震. (民國 91 年) 過氧化酵素之製備及酵素固定化, *國立交通大學. 碩士論文*.
45. 吳岳縉. (民國 91 年) *Coprinus cinereus* 過氧化氫酵素於大腸桿菌中之表現及特性研究, *國立交通大學. 碩士論文*.
46. 呂佩怡. (民國 89 年) 建立快速檢測生物胺類化合物之系統, *國立交通大學. 碩士論文*.
47. Gallati, H. (1979) Horseradish peroxidase: a study of the kinetics and the determination of optimal reaction conditions, using hydrogen peroxide and 2,2'-azinobis 3-ethylbenzthiazoline-6-sulfonic acid (ABTS) as substrates, *J. Clin. Chem. Clin. Biochem. 17*, 1-7.
48. Metelitsa, D. I., Arapova, G. S., Vidzhinaite, R. A., Demcheva, M. V., Litvinchuk, A. V., and Razumas, V. I. (1994) Co-oxidation of phenols and 4-aminoantipyrene catalyzed by microperoxidase and their complexes with proteins, *Biokhi. (Moscow, Russia) 59*, 1285-1298.
49. Anthon, G. E., and Barrett, D. M. (2001) Colorimetric method for the determination of lipoxygenase activity, *J. Agric. Food. Chem. 49*, 32-37.

50. Nicell, J. A., and Wright, H. (1997) A model of peroxidase activity with inhibition by hydrogen peroxide, *Enzyme Microb. Technol. 21*, 302-310.
51. Tams, J. W., and Welinder, K. G. (1996) Unfolding and refolding of *Coprinus cinereus* peroxidase at high pH, in urea, and at high temperature. Effect of organic and ionic additives on these processes, *Biochem. 35*, 7573-7579.
52. Hushpulian, D. M., Savitskip, A., Rojkova, M., Chubar, T. A., Fechina, V. A., Sakharov, I. Yu., Lagrimini, L. M., Tishkov, V. I. and Gazaryan, I. G. (2003) Expression and Refolding of Tobacco Anionic Peroxidase from E. coli Inclusion Bodies *Biochem. (Moscow) 68*, 1189-1194.
53. Hahn, H. S., Park, Y. D., Lee, J. R., Park, K. H., Kim, T. J., Yang, J. M., and Hahn, M. J. (2003) Aggregation and folding of recombinant human creatine kinase, *J. Protein Chem. 22*, 563-570.
54. Gazaryan, I. G.., Doseeva, V. V., Galkin, A. G., and Tishkov, V. I. (1994) Effect of single-point mutations Phe41-->His and Phe143-->Glu on folding and catalytic properties of recombinant horseradish peroxidase expressed in *E. coli*, *FEBS Lett. 354*, 248-250.
55. Whitwam, R., and Tien, M. (1996) Heterologous expression and reconstitution of fungal Mn peroxidase, *Arch. Biochem. Biophys. 333*, 439-446.
56. Kim, B. B., Pisarev, V. V., and Egorov, A. M. (1991) A comparative study of peroxidases from horse radish and *Arthromyces ramosus* as labels in luminol-mediated chemiluminescent assays, *Anal. Biochem. 199*, 1-6.
57. Sutherland, G. R., Zapanta, L. S., Tien, M., and Aust, S. D. (1997) Role of calcium in maintaining the heme environment of manganese peroxidase, *Biochem. 36*, 3654-3662.
58. Liu, J. Z., Wang, T. L., Huang, M. T., Song, H. Y., Weng, L. P., and Ji, L. N. (2006) Increased thermal and organic solvent tolerance of modified horseradish peroxidase, *Protein Eng. Des. Sel. 19*, 169-173.
59. Pina, D. G., Shnyrova, A. V., Gavilanes, F., Rodriguez, A., Leal, F., Roig, M. G., Sakharov, I. Y., Zhadan, G. G., Villar, E., and Shnyrov, V. L. (2001) Thermally induced conformational changes in horseradish peroxidase, *Eur. J. Biochem. 268*, 120-126.
60. Kamal, J. K., Nazeerunnisa, M., and Behere, D. V. (2002) Thermal unfolding of soybean peroxidase. Appropriate high denaturant concentrations induce cooperativity allowing the correct measurement of thermodynamic parameters, *The J. Biol. Chem. 277*, 40717-40721.
61. Rodriguez, A., Pina, D. G., Yelamos, B., Castillo Leon, J. J., Zhadan, G. G., Villar, E., Gavilanes, F., Roig, M. G., Sakharov, I. Y., and Shnyrov, V. L. (2002) Thermal stability of peroxidase from the african oil palm tree Elaeis guineensis, *Eur. J. Biochem. 269*, 2584-2590.

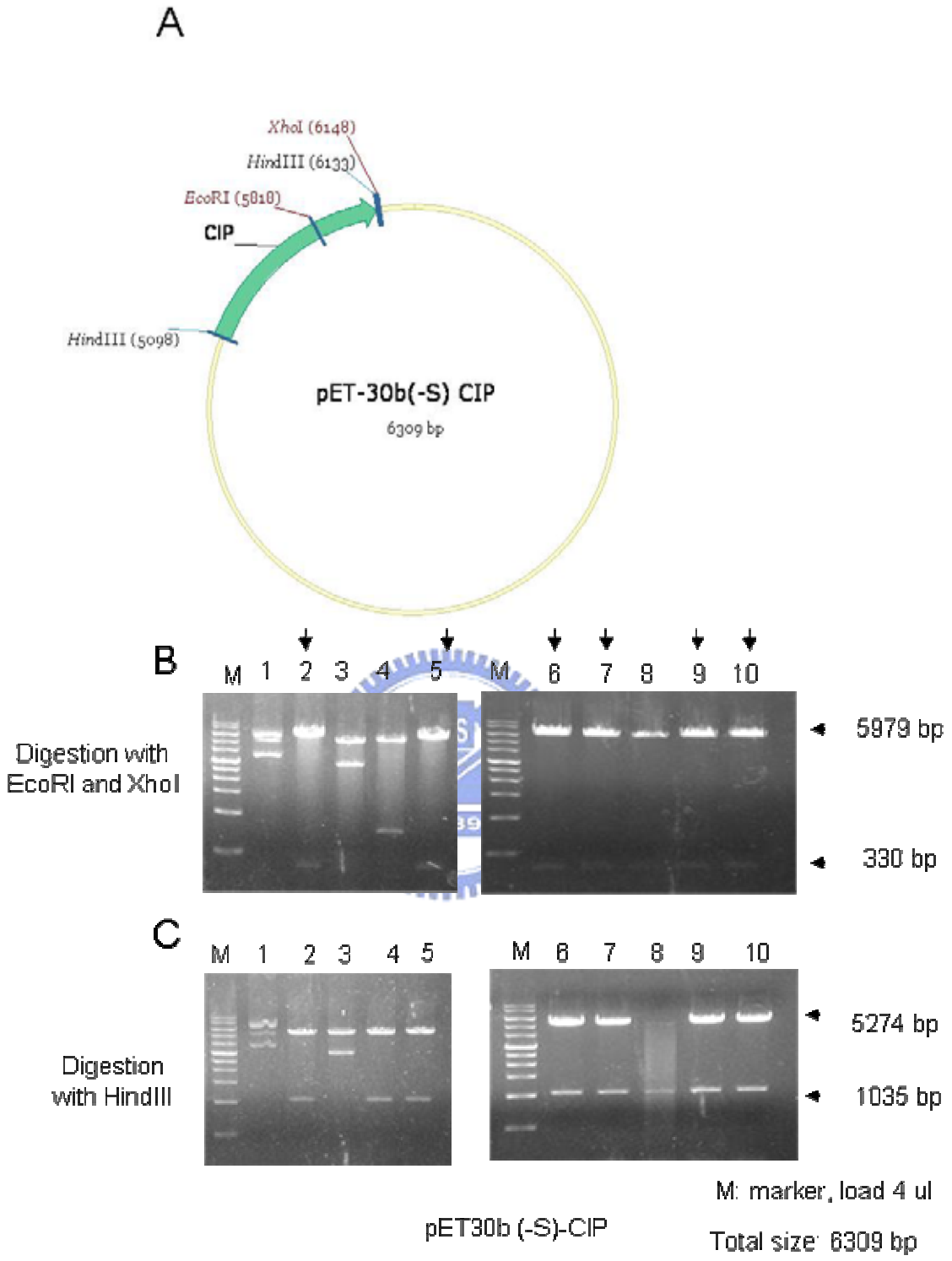

Fig. 1 The diagram of constructed pET30b(-S)-CIP vector.

(A) Plasmid diagram of pET30b(-S)-CIP (6309 bp). The pET 30b(-S)-CIP vector was digested with EcoRI and XhoI (B) or with Hind III (C). M, marker. Lane 2, lane 5, lane 6, lane 7, lane 9 and lane 10 : pET30b(-S)-CIP vector.

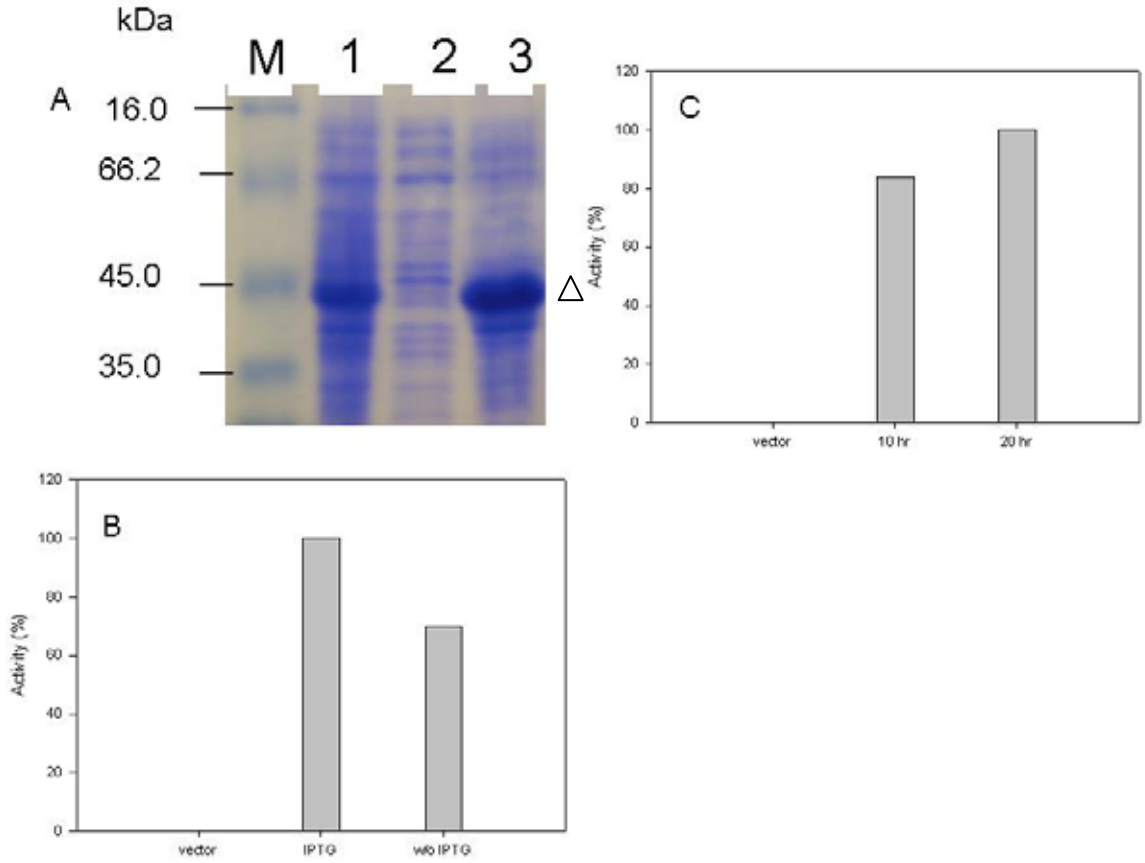

Fig. 2 Expression of recombinant CIP under different conditions.

(A) 10 % SDS-PAGE of E. coli cells after 50 μM IPTG induction for 10 h. The total cell lysate (lane 1), supernatant (lane2), and pellet (lane3) were resolved on a 10 % SDS-PAGE. △, recombinant CIP. (B) The effect of IPTG (50 μM). (C) The effect of inducing time (10 and 20 h).

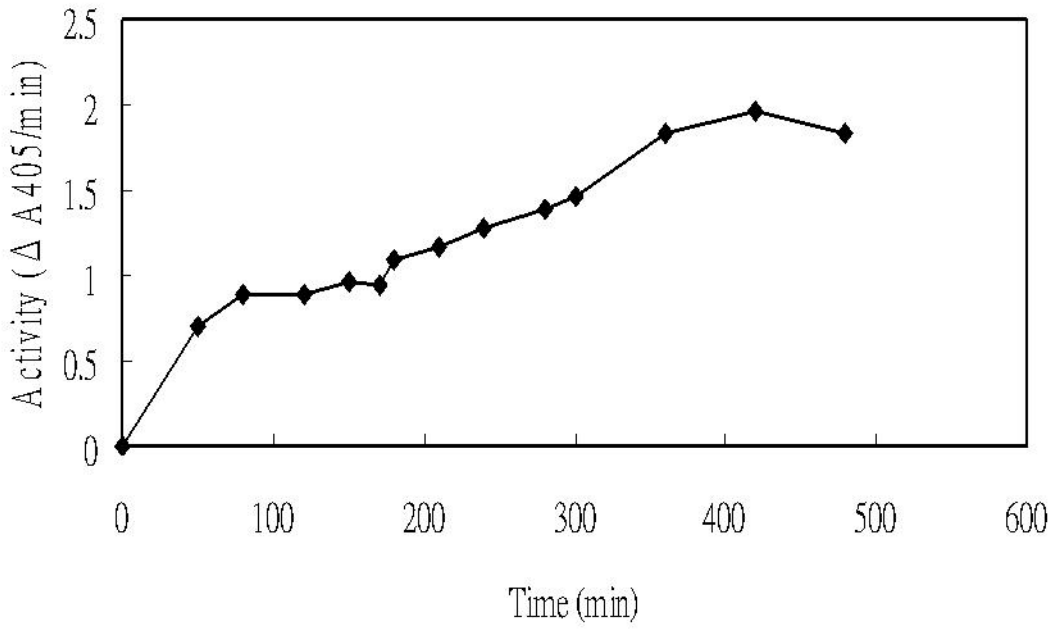

Fig. 3 The time-dependent renaturation of recombinant CIP.

The enzyme was renatured in the presence of 5 mM $CaCl_2$, 5 μM hemin, 1.8 M urea, 0.5 mM oxidized glutathione, 0.1 mM DTT, and 5 % glycerol in 50 mM Tris-HCl buffer (pH 9.5) and assayed directly without dialysis and purification at the indicated times. Activity assay was performed in the presence of 0.05 mg/ml protein, 0.5 mM ABTS, and 5 mM H_2O_2 in 100 mM sodium acetate, pH 5.2.

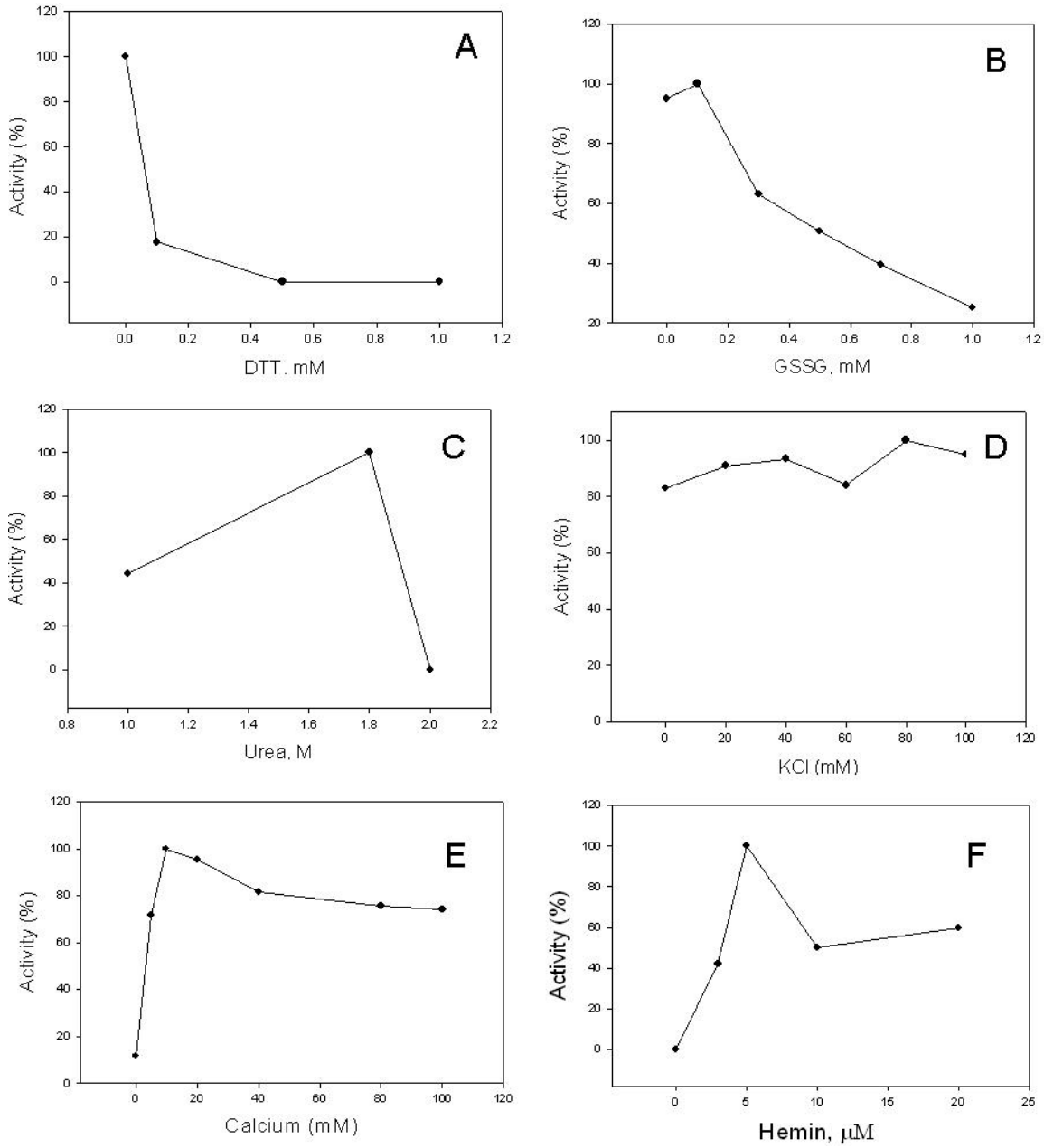

Fig. 4 The effect of various agents on the refolding of recombinant CIP.

The effect of concentrations of DTT (0.1, 0.5 and 1.0 mM) (A), GSSG (0, 0.1, 0.3, 0.5, 0.7 and 1.0 mM) (B), urea (1.0, 1.8 and 2.0 mM) (C), KCl (0, 20, 40, 60, 80 and 100 mM) (D), calcium (0, 5, 10, 20, 40, 80 and 100 mM) (E) or hemin (0, 3, 5, 10 and 20 μM) (F) in the reactivation of CIP were tested. After reactivation, the activity of recombinant CIP was assayed as indicated in Fig. 3.

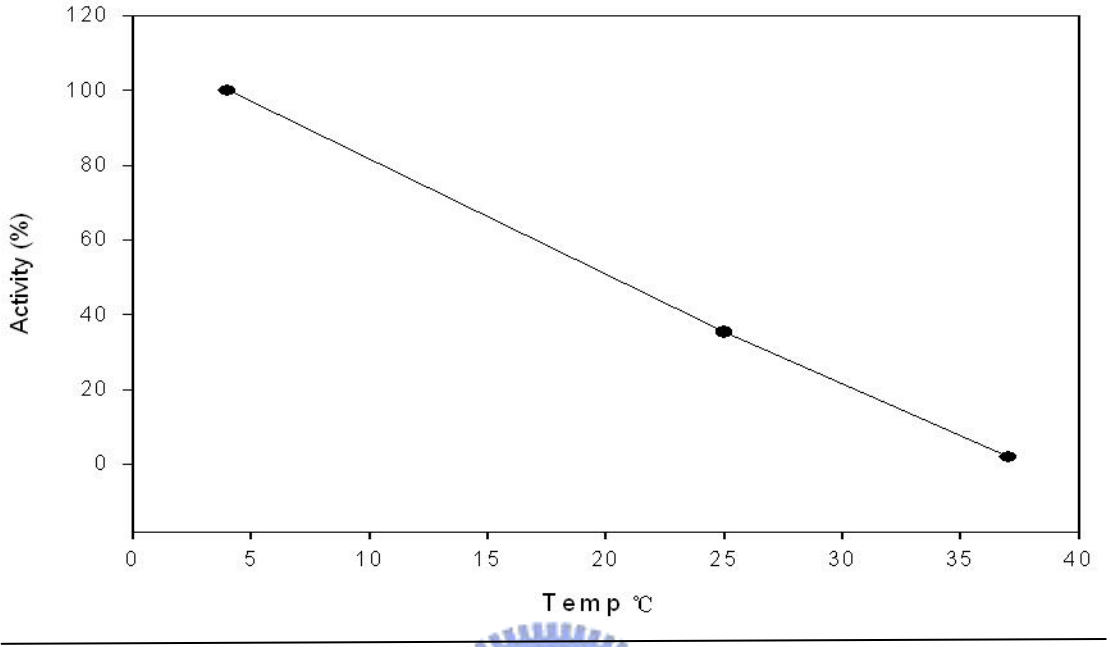

Fig. 5 The effect of temperature on the renaturation of recombinant CIP.

The enzyme was renatured in the presence of 5 mM $CaCl_2$, 5 μM hemin, 1.8 M urea and 5 % glycerol in 50 mM Tris-HCl buffer (pH 9.5). Activity assay was performed in the presence of 0.05 mg/ml protein, 0.5 mM ABTS, and 5 mM H_2O_2 in 100 mM sodium acetate pH 5.2.

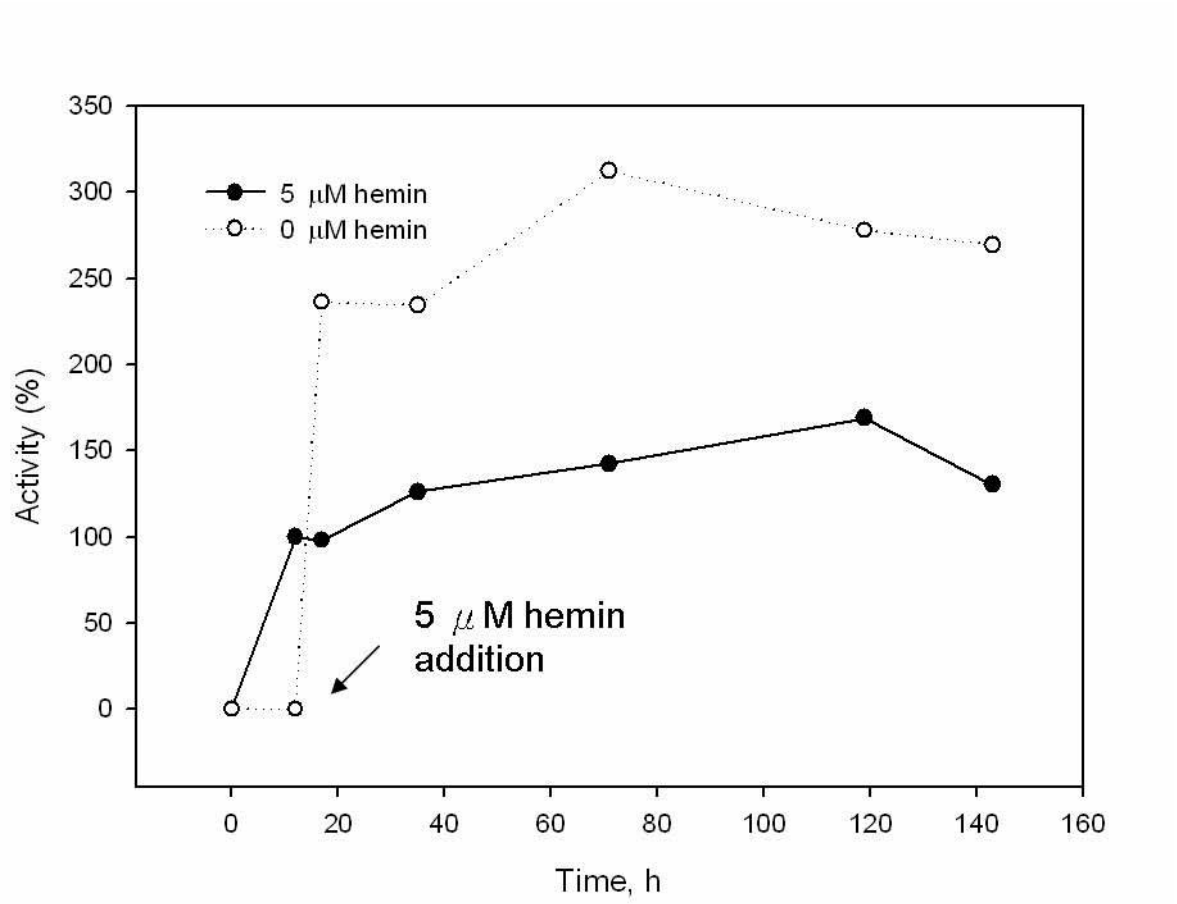

Fig. 6 The effect of hemin in the renaturation of recombinant CIP.

The enzyme was renatured in 50 mM Tris-HCl buffer (pH 9.5) containing 5 mM $CaCl_2$, 1.8 M urea, 5 % glycerol and with or without 5 μM hemin. After renaturation for 12 h, 5 μM hemin was added to the refolded recombinant CIP without hemin. At indicated times refolded CIP was withdrawn and subjected to activity assay. The activity was monitored at 405 nm.

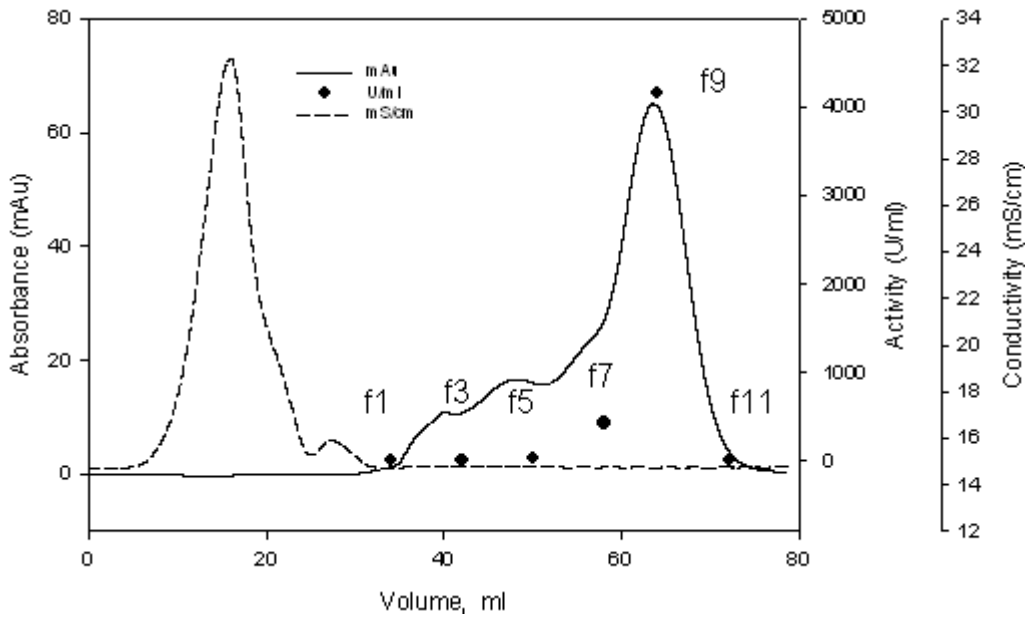

Fig. 7-1 Elution profile of the recombinant CIP on the first gel filtration column (S-200). The protein was eluted in a flow rate of 0.5 mL/min by 50 mM Tris-HCl containing 150 mM NaCl, pH 8.5. Each fraction was collection in a volume of 4 mL/fraction.

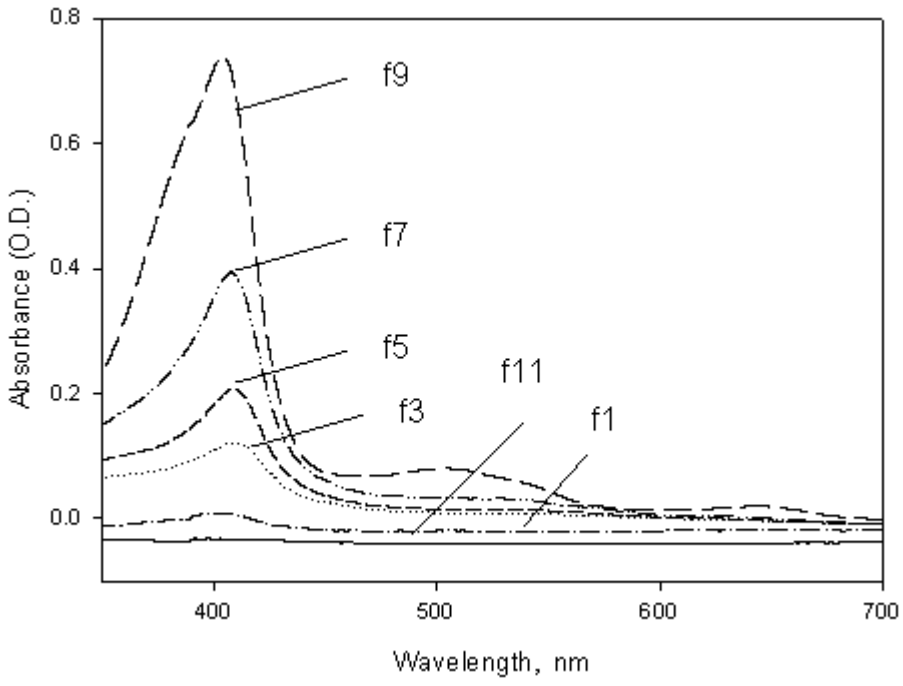

Fig. 7-2 Absorption spectra between 350 and 700 nm of the indicated fractions from the first gel-filtration column (S-200) (Fig. 7-1).

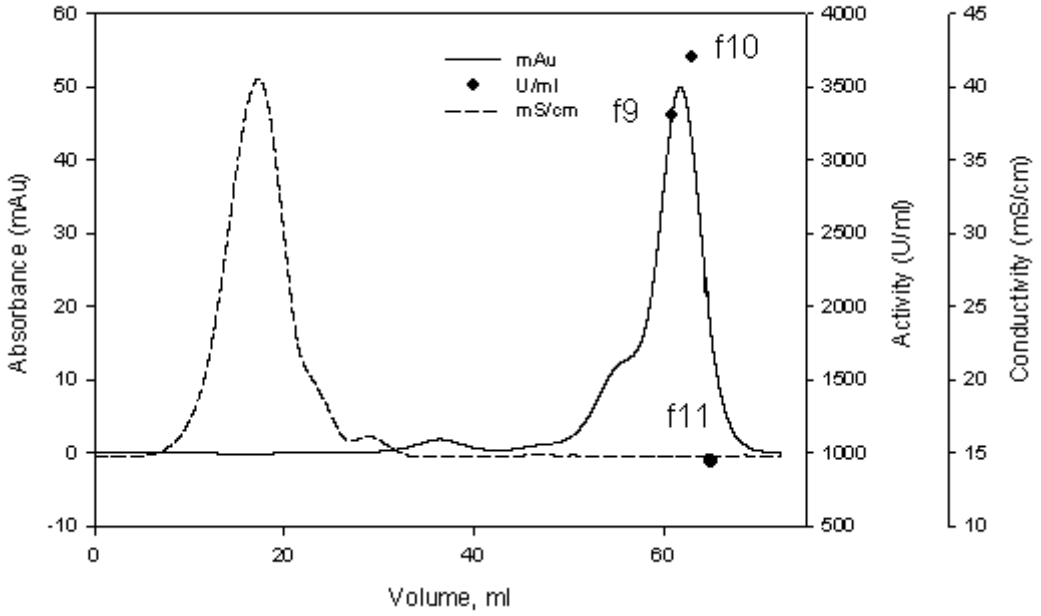

Fig. 8-1 Elution profile of the recombinant CIP on the second gel filtration column (S-200). The protein was eluted in a flow rate of 0.5 mL/min by 50 mM Tris-HCl containing 150 mM NaCl, pH 8.5. Each fraction was collection in a volume of 4 mL/fraction for fractions 1-9 and 2 mL/fraction for fractions 9-11.

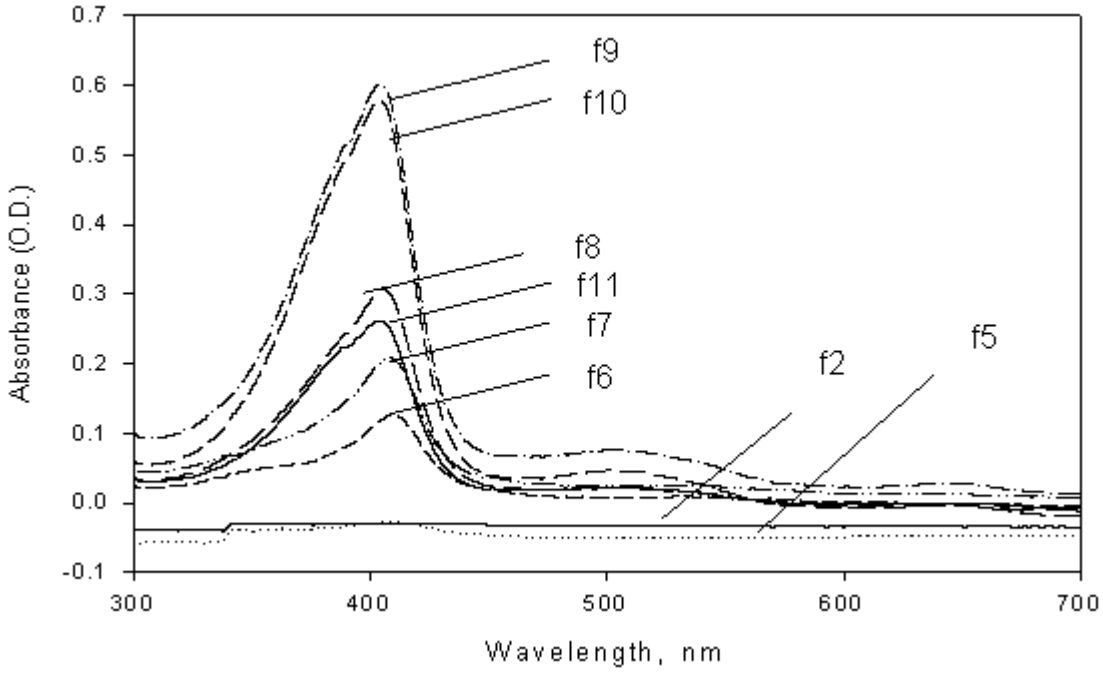

Fig. 8-2 Absorption spectra between 300 and 700 nm of the indicated fractions from the second gel-filtration column (S200) (Fig. 8-1).

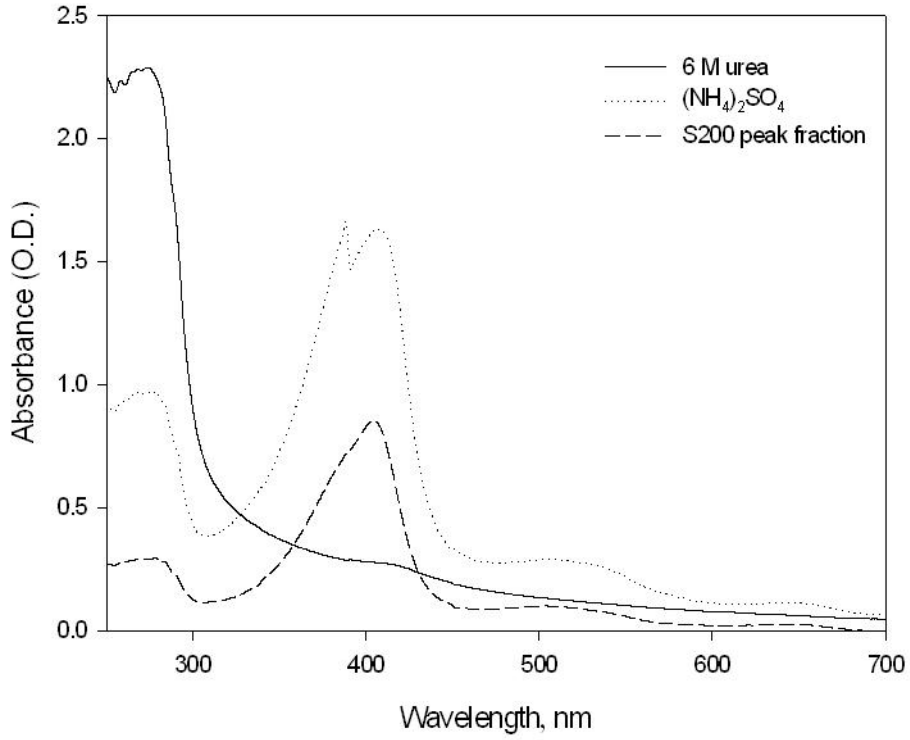

Fig. 9 Absorbance spectra between 250 and 700 nm of recombinant CIP from different stages during purification.

Spectrum of CIP in 6 M urea is shown as solid line; Spectrum of CIP after ammonium sulfate precipitation is shown as dotted line and spectrum of fraction 9 from column S-200 (Fig. 8-1) as shown as dashed line.

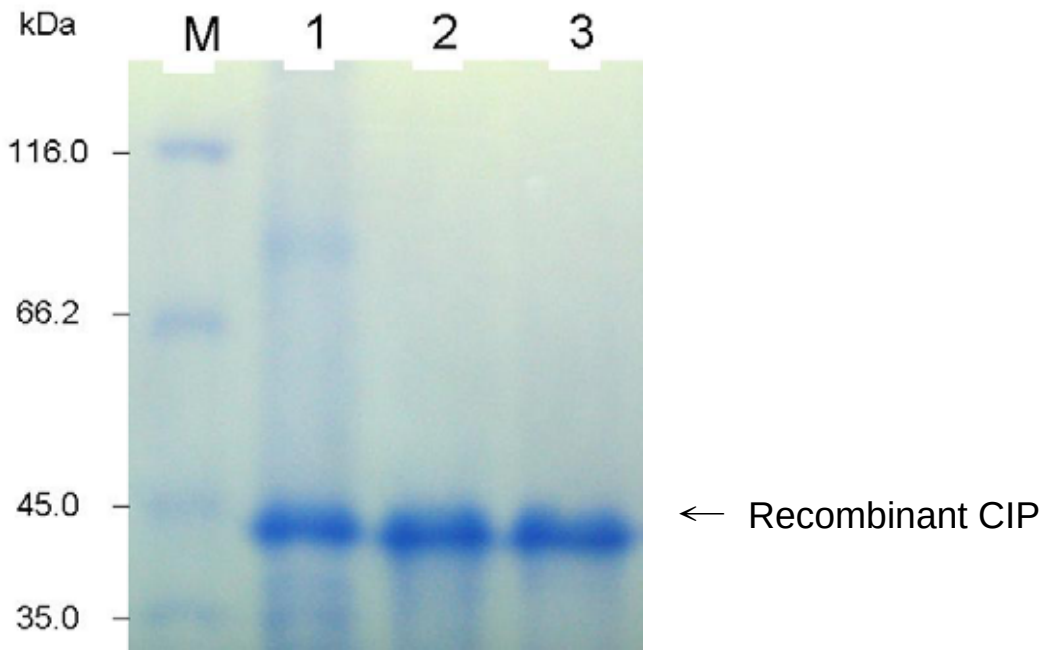

Fig. 10 SDS-PAGE of purified recombinant CIP.

The inclusion body (Lane 1), fraction 9 of first gel filtration S200 in Fig. 7-1 (Lane 2), and fraction 10 from second gel filtration in Fig. 8-1 (Lane 3) were resolved on a 10 % SDS-PAGE, followed by staining with coomassie blue.

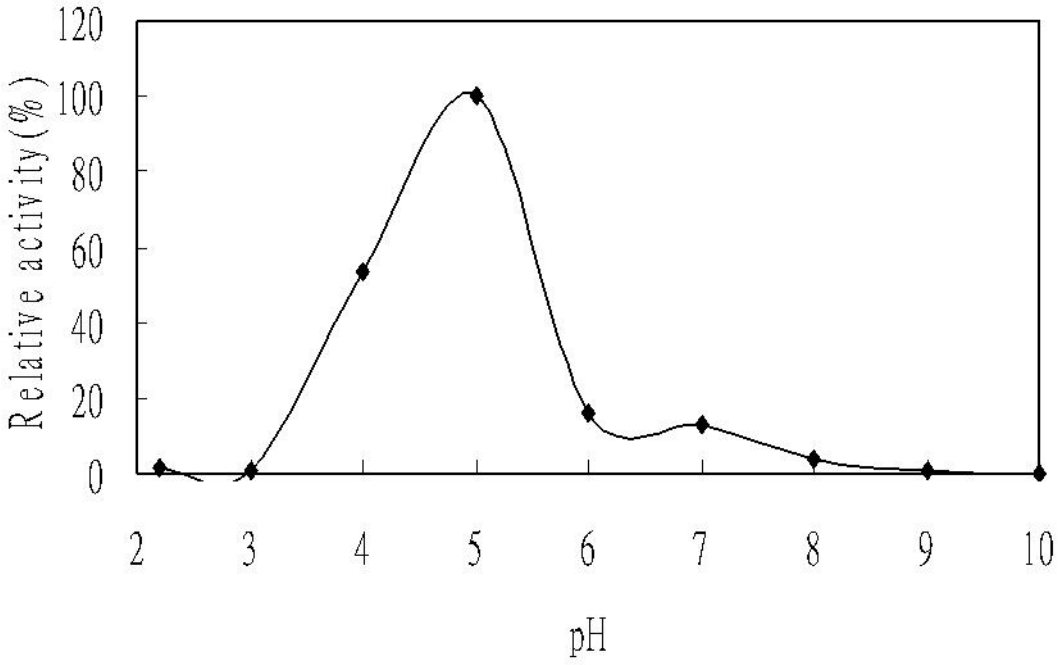

Fig. 11 The optimal pH of catalytic activity for recombinant CIP.

The reactivity of recombinant CIP to ABTS under different pH. CIP (0.068 U) in reaction mixture of different pHs (pH 2.2-10) in the presence of 0.5 mM ABTS and 5 mM H_2O_2 in buffers of different pHs. The buffers used were: 0.2 M Gly-HCl at pH 2.2-3; 0.2 M sodium acetate at pH 4-5; 0.2 M K-phosphate at pH 6-8; 0.2 M Tris-HCl at pH 9-10.

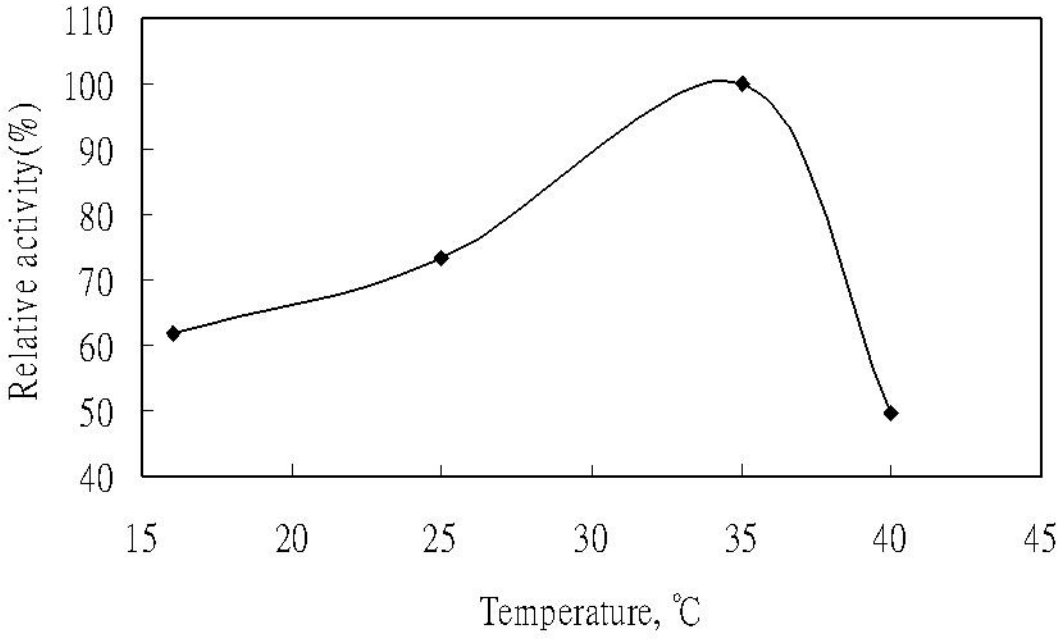

Fig. 12 Effect of temperature on the catalytic activity of recombinant CIP.

Reaction was performed in a reaction mixture containing 0.068 U CIP, 0.5 mM ABTS, 5 mM H_2O_2, and 100 mM sodium acetate , pH 5.2 at different temperature (15 ℃, 25 ℃, 35 ℃ and 40 ℃) for 1 min.

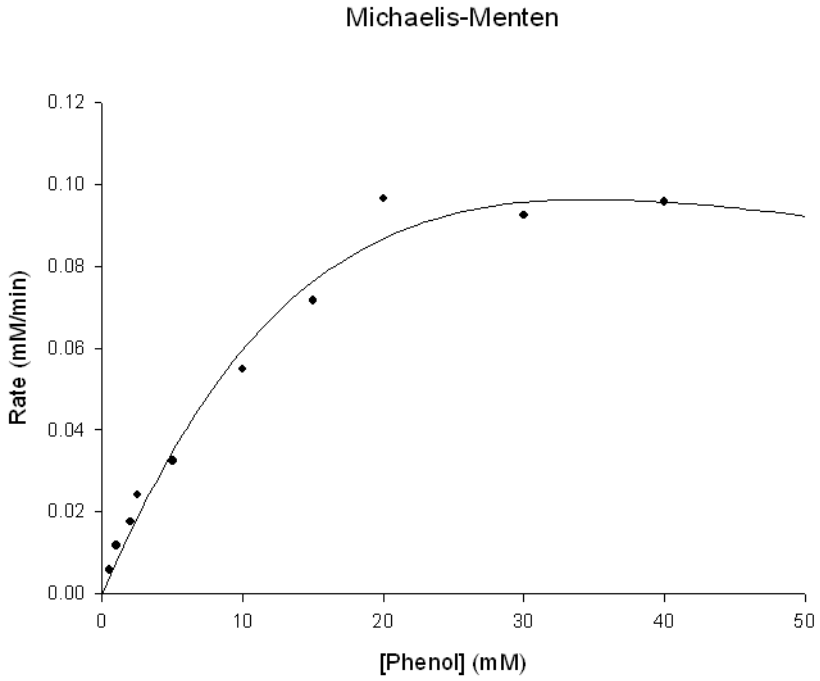

Fig. 13-1 Kinetics study of recombinant CIP using phenol and H_2O_2 as substrates. Activities were determined in 100 mM phosphate buffer, pH 7.4 containing 0.2 mM H_2O_2, 2.4 mM 4-AAP (4-aminoantipyrine), 0.043 U recombinant CIP, and various concentrations of phenol (0.5-40 mM) at 25 ℃. Activity was monitored on spectrophotometer (Hitachi U3010) at O.D. 510 nm.

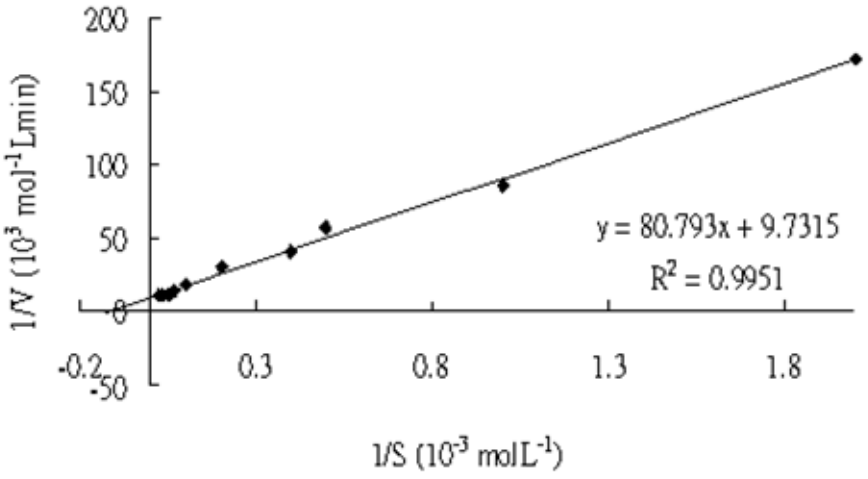

Fig. 13-2 Double reciprocal plot of data derived from Fig. 13-1.

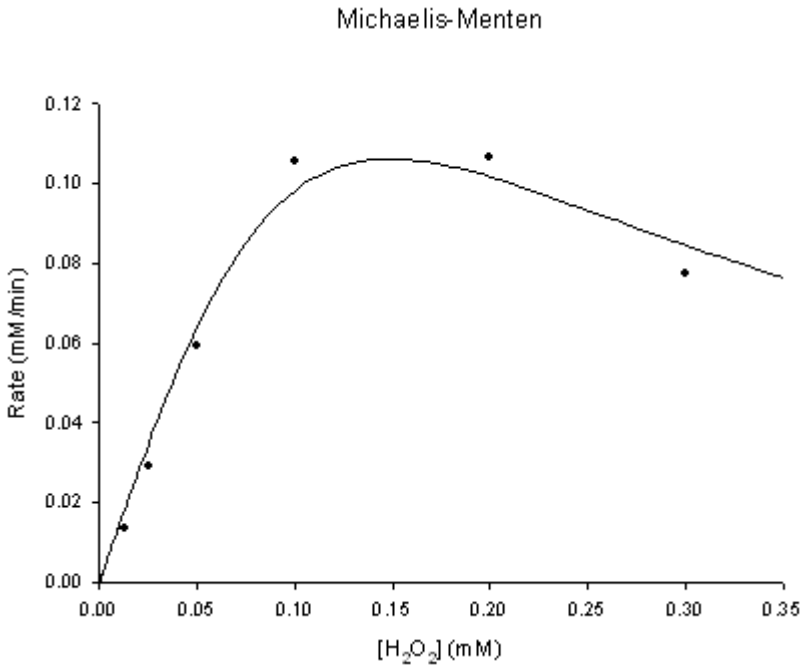

Fig. 14-1 Kinetics study of recombinant CIP by using phenol and H_2O_2 as substrates. The reaction mixture is composed of 10 mM phenol, 0.043 U recombinant CIP in 100 mM phosphate buffer, pH 7.4 containing various concentrations of H_2O_2 (0.0125-0.3 mM) at 25 ℃. Activity was monitored on spectrophotometer (Hitachi U3010) at O.D. 510 nm.

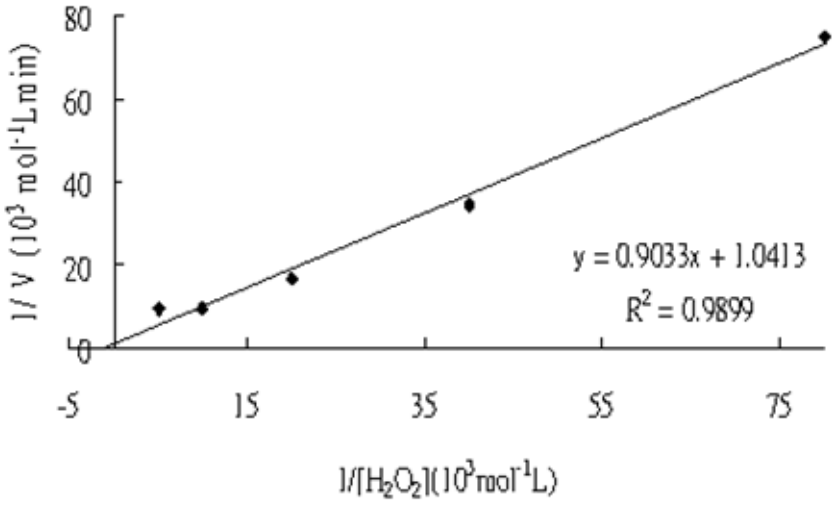

Fig. 14-2 Double reciprocal plot of data derived from Fig. 14-1.

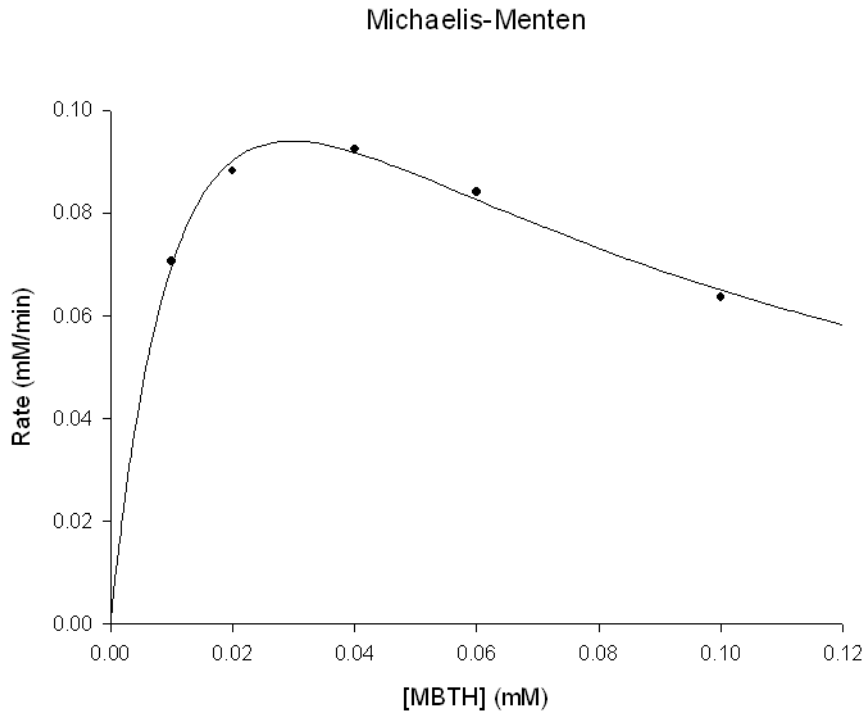

Fig. 15-1 Kinetics study of recombinant CIP by using MBTH and H_2O_2 as substrates. Activities were determined in 200 mM phosphate-citrate buffer (400 mM NaH_2PO_4/200 mM $Na_3C_6H_5O_7$), pH 4.0 containing 0.4 mM H_2O_2, 2 mM DMAB, 0.037 U recombinant CIP and various concentrations of MBTH (0.01-0.1 mM) at 25 ℃. Activity was monitored on spectrophotometer (Hitachi U3010) at O.D. 590 nm.

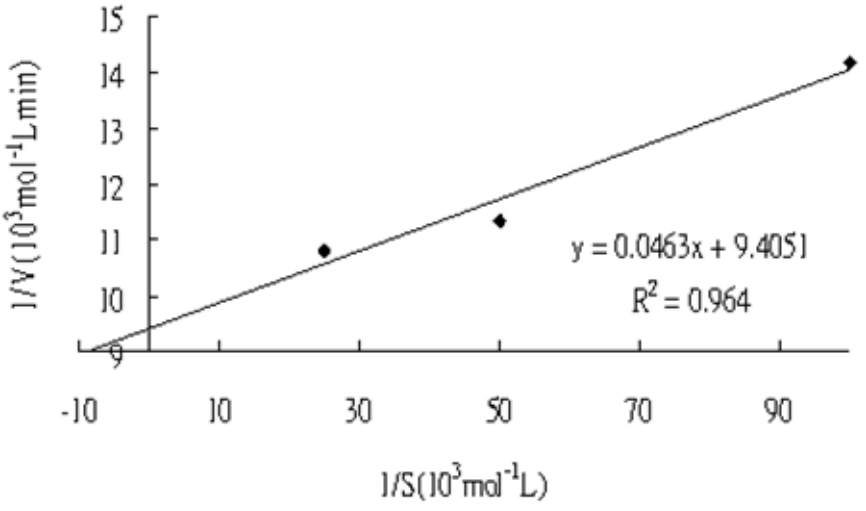

Fig. 15-2 Double reciprocal plot of data derived from Fig. 15-1.

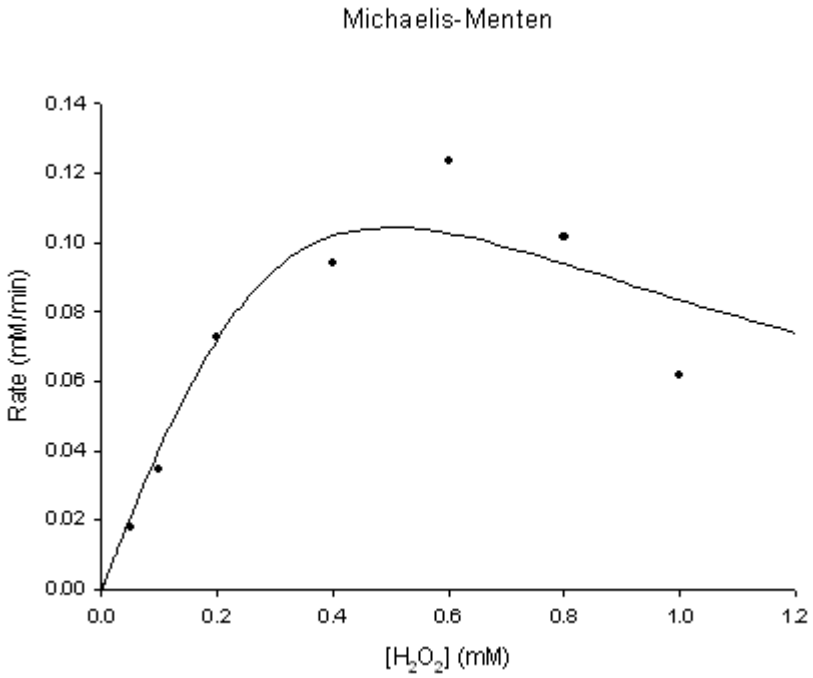

Fig. 16-1 Kinetics study of recombinant CIP by using H_2O_2 and MBTH as substrates. The mixture was composed of 2 mM DMAB, 0.037 U recombinant CIP, 0.04 mM MBTH in 200 mM phosphate-citrate buffer (400 mM NaH_2PO_4/200 mM $Na_3C_6H_5O_7$), pH 4.0 containing various concentrations of H_2O_2 (0.05-1.0 mM) at 25 ℃. Activity was monitored on spectrophotometer (Hitachi U3010) at O.D. 590 nm.

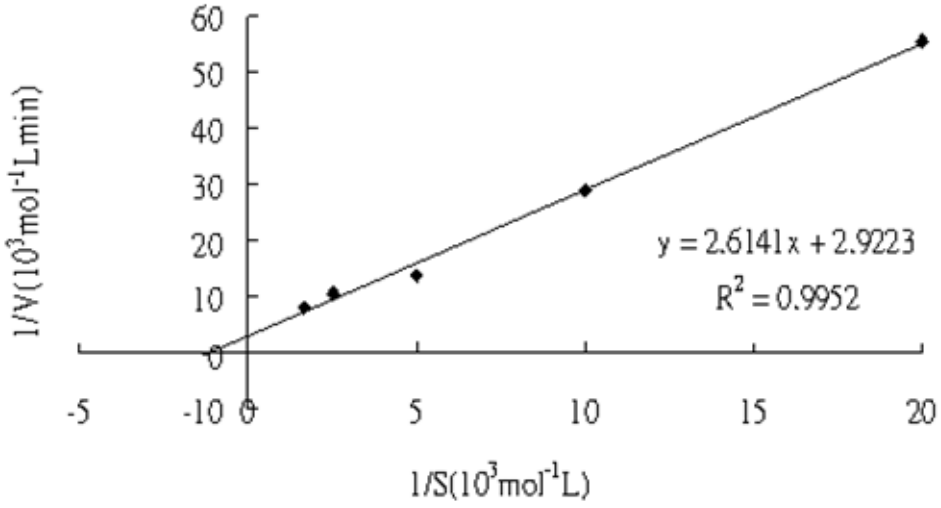

Fig. 16-2 Double Reciprocal plot of data derived from Fig. 16-1.

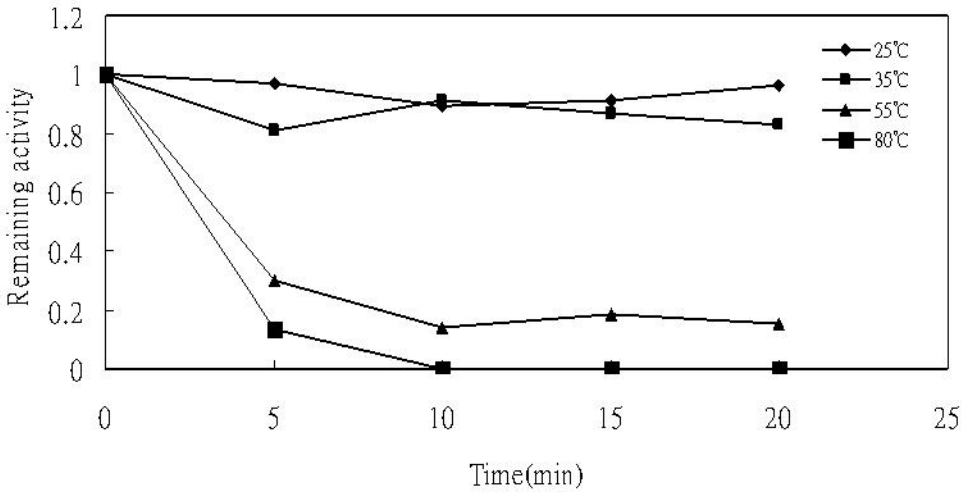

Fig. 17 Thermostability of recombinant CIP.

Recombinant CIP (10 μL, 63.2 U) was incubated at 25 ℃, 35 ℃, 55 and 80 ℃ for 5-20 min. At the indicated times, an aliquot CIP solution (1 μL, 0.06 U) was taken out, cooled on ice and subjected to activity assay. Activity assay was performed with 0.06 U recombinant CIP, 5 mM H_2O_2, 0.5 mM ABTS, 100 mM sodium acetate (pH 5.2) at 25 ℃. The remaining activity of recombinant CIP was determined at O.D. 405 nm.

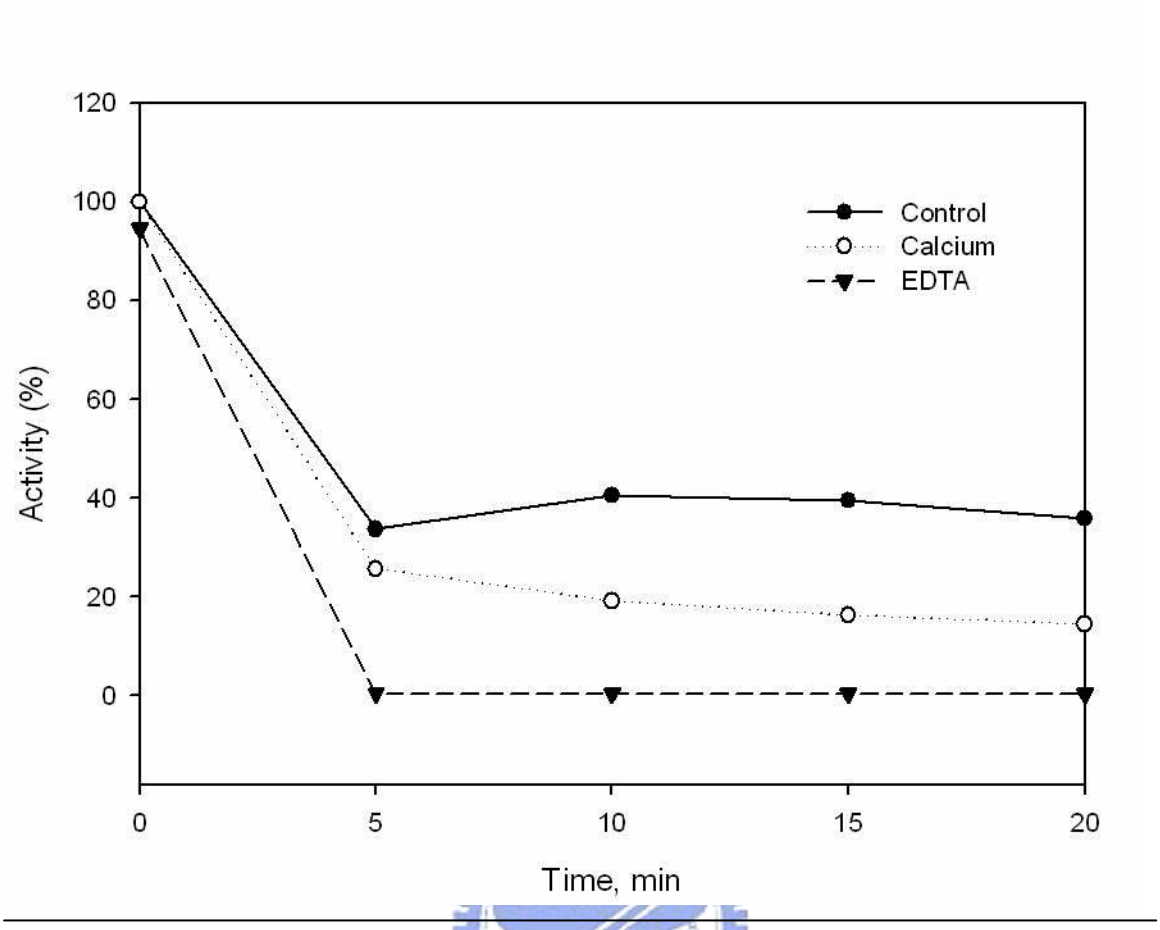

Fig. 18 Effect of calcium and EDTA on the thermostability of CIP.

Recombinant CIP (10 μL, 63.2 U) was incubated at 55 ℃ in 50 mM Tris-HCl buffer (pH 8) in the presence of 1 mM EDTA or 1 mM $CaCl_2$. At the indicated times, an aliquot of CIP (1 μL, 0.06 U) was taken out, cooled on ice and subjected to activity assay. The assay mixture was composed of 0.064 U recombinant CIP, 5 mM H_2O_2, 0.5 mM ABTS, 100 mM sodium acetate (pH 5.2) at 25 ℃ for 1 min.

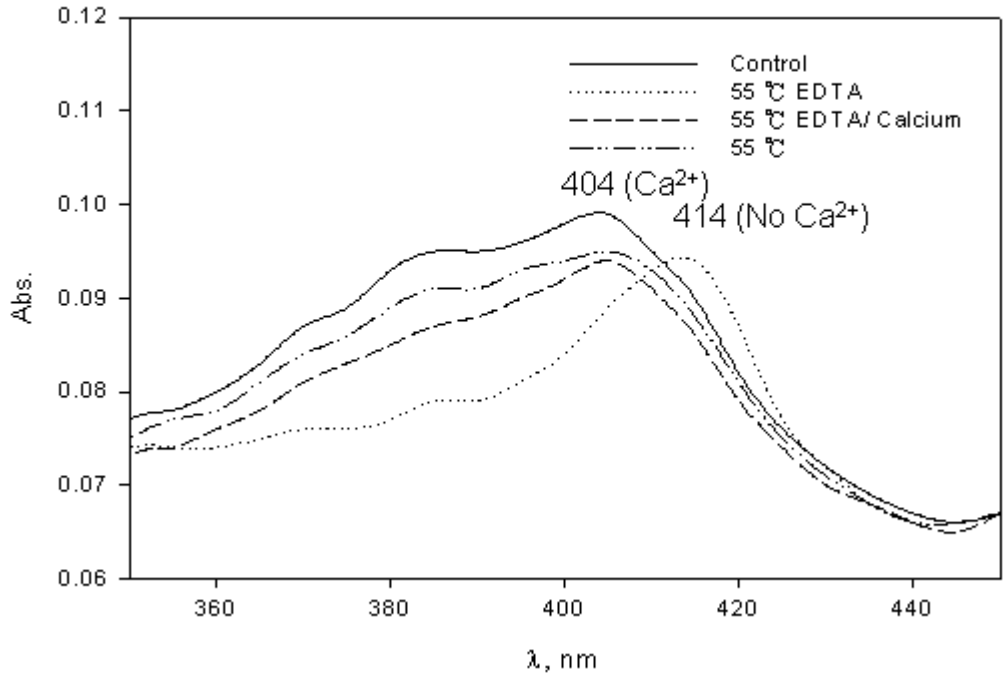

Fig. 19 Absorption spectra of recombinant CIP before and after heat treatment with different ligands.

Recombinant CIP (30 μL, 207.6 U) was untreated (—), treated at 55 ℃ for 5 min (-··), treated at 55 ℃ in the presence of 1 mM EDTA for 5 min (…) and treated with 1 mM $Ca^{2+}$and 1mM EDTA at 55 ℃ for 5 min (---). After incubation, 270 μL of 50 mM Tris-HCl buffer, pH 8.0, was added to the enzyme solution with a total volume of 300 μL, and scan on Hitachi U3010 between wavelengths 350 nm and 450 nm. Hemin in pyridine exhibits peak absorption of 388 nm.

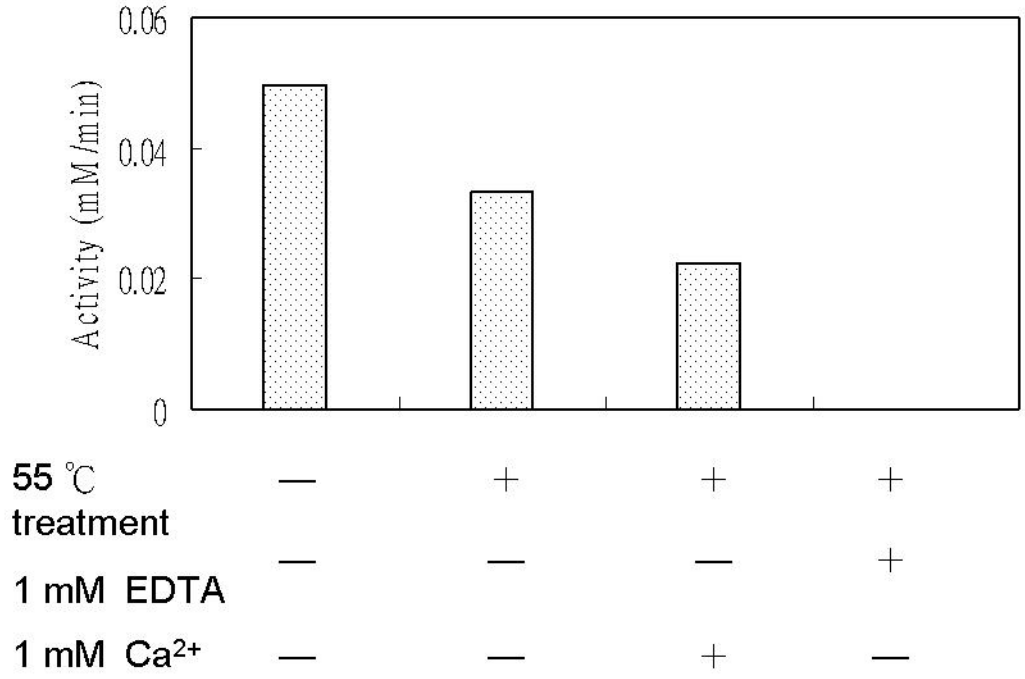

Fig. 20 Effects of calcium and EDTA on the heat inactivation of recombinant CIP. Recombinant CIP (30 μl, 207.6 U) was incubated in 50 mM Tris-HCl buffer (pH 8.0) at 55 ℃ without or with 1 mM EDTA or 1mM Ca^{2+} for 5 min. The activity was determined by incubating 0.068 U heat treated recombinant CIP in 100 mM sodium acetate, pH 5.2 containing 5 mM H_2O_2 and 0.5 mM ABTS at 25℃ for 1 min.

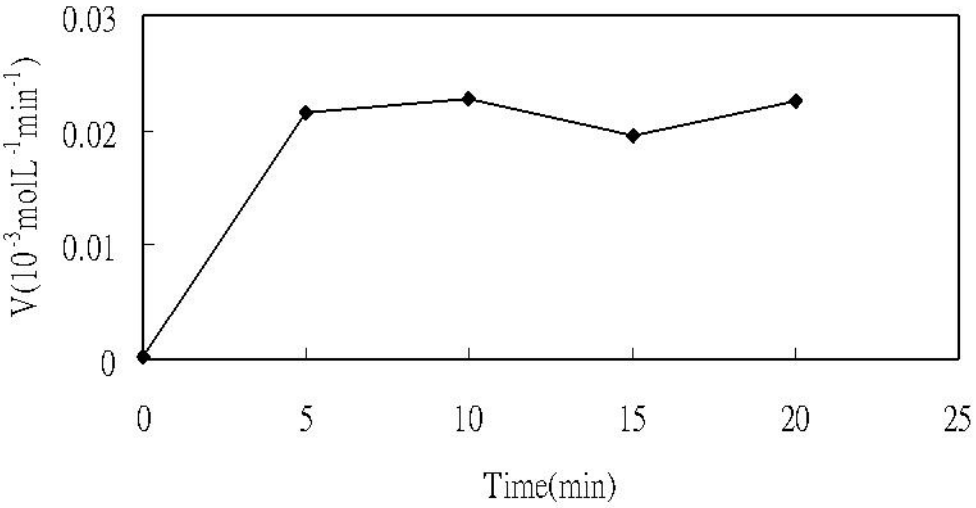

Fig. 21 Effect of Ca^{2+} ion on the renaturation of recombinant CIP.

Recombinant CIP (207.6 U) in 30 μL of 50 mM Tris-HCl buffer, pH 8.0, containing 1 mM EDTA was incubated at 55 ℃ for 5 min. Refolding was performed by adding Ca^{2+} to a final concentration of 1 mM and incubating at 4 ℃ for 0-20 min. The assay mixture was composed of 0.068 U recombinant CIP, 5 mM H_2O_2, 0.5 mM ABTS, in 100 mM sodium acetate, pH 5.2 at 25 ℃ for 1 min. The resulting activity was monitored on Hitachi U3010 spectrophotometer at O.D. 510 nm.

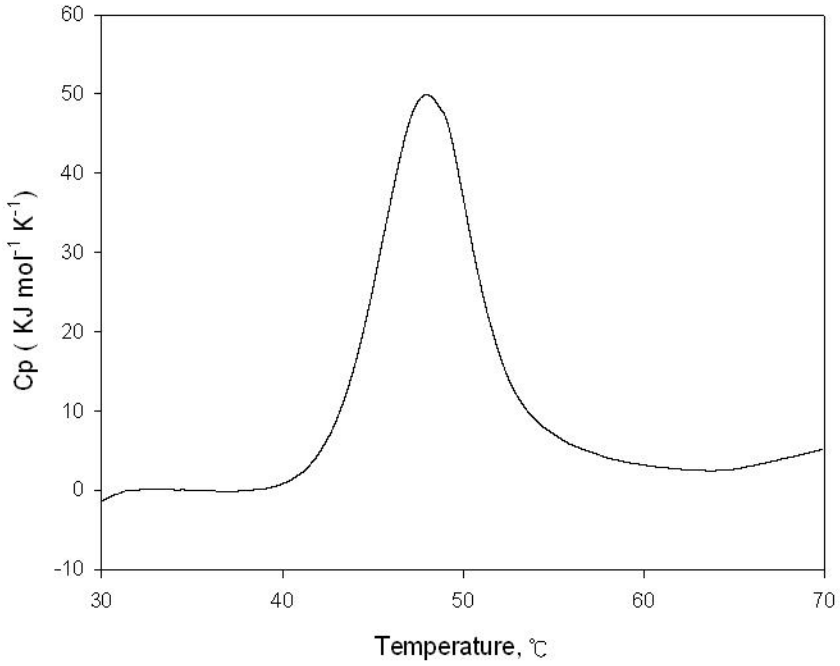

Fig. 22 Differential scanning calorimetry (DSC) analysis of recombinant CIP.

Recombinant CIP (500 μL, 1 mg/mL) was scanned in a rate of 1 K/min to study the phase transition with increasing temperature from 30 ℃ to 70 ℃. An over-pressure of 3 atm was maintained over the liquid in the cells throughout the scan. Measurement showed a peak with a transition temperature of 48 ℃. The area under the DSC curve corresponds to the molar enthalpy change ΔH_{cal} for the phase transition.

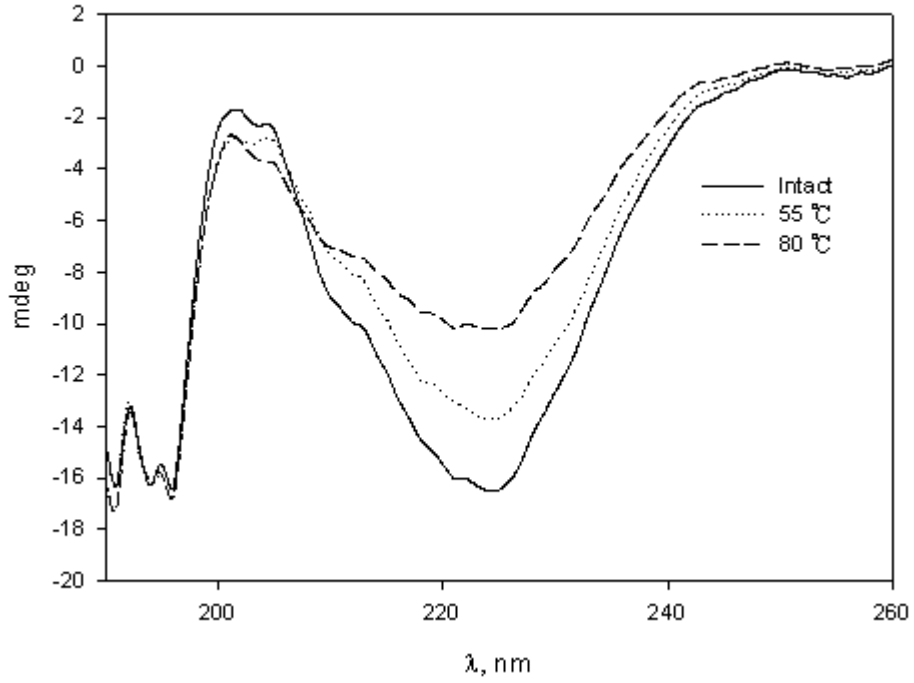

Fig. 23 CD spectra of recombinant CIP in the far-ultraviolet region.

CD spectra of recombinant CIP in the far-ultraviolet region (190-260 nm) of untreated (solid line) , treated at 55 ℃ for 10 min (dotted line), or at 80 ℃ for 10 min (dashed line) were recorded. CIP (2106.1 U, 300 μL) was incubated at 55 ℃ or 80 ℃ for 10 min prior to the CD analysis in the far-UV region (190-260 nm). A cell with 1 mm path length was used during recording CD spectra reported in this study were an average of sixteen scans at a speed of 200 nm/min

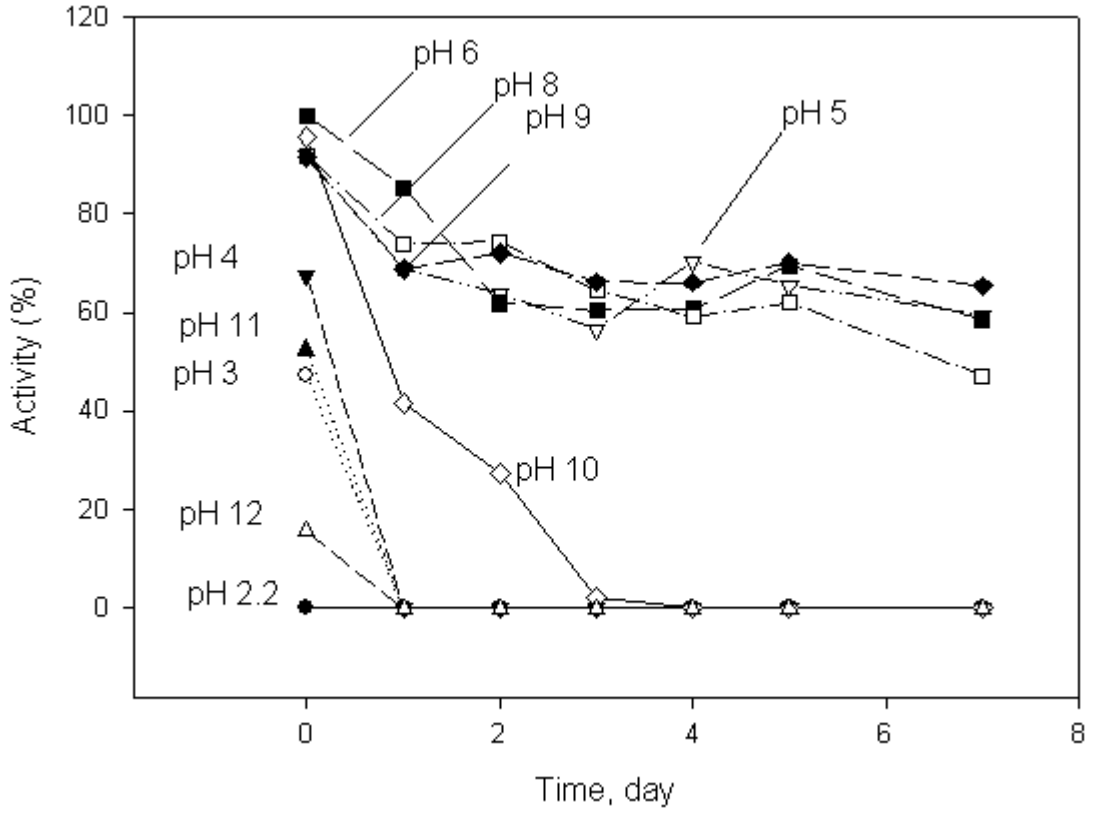

Fig. 24 The long term stability of recombinant CIP under different pH values.

Recombinant CIP (207.6 U/300 μL) was incubated at different pH (2.2-12) at 25 ℃ for a 7-day period. At the indicated times, an aliquot enzyme solution (1 μL) was taken out for enzyme activity assay. Activity Assay was carried out by incubating 0.068 U recombinant CIP with reaction mixture (5 mM H_2O_2, 0.5 mM ABTS in 100 mM sodium acetate, pH 5.2) at 25℃ for 1 min. The activity was determined at O.D. 405 nm.

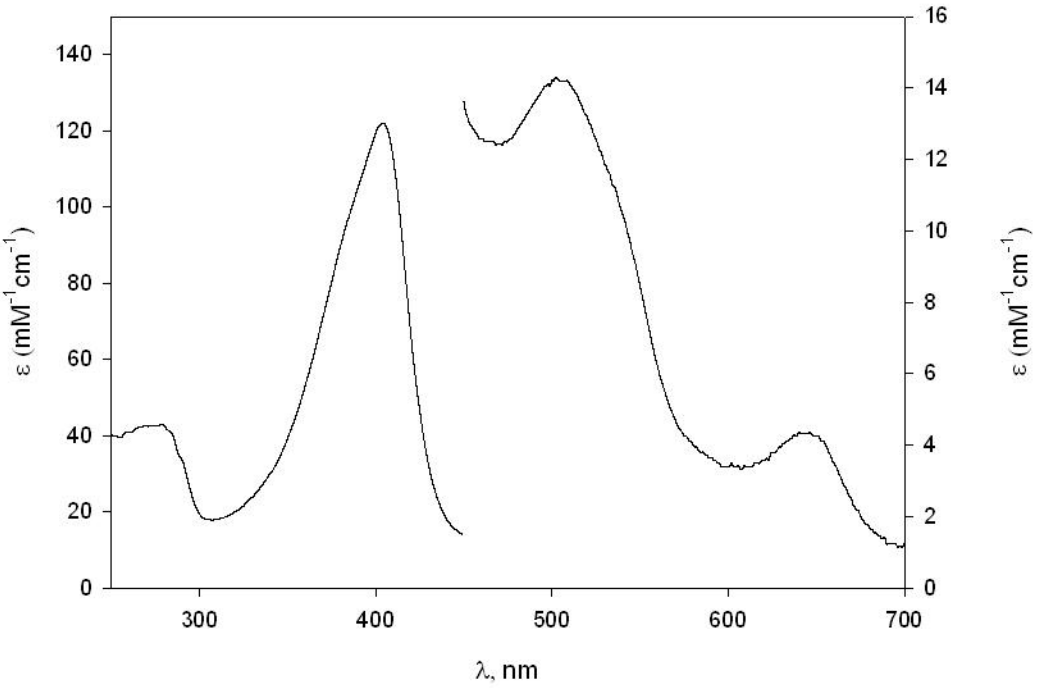

Fig. 25 Absorption spectra of recombinant CIP (7 μM) between wavelengths of 700 nm and 250 nm.

Table 1. Reactivation of recombinant CIP under different conditions.

Purification steps	specific activity (U/mg)	
	w/o GSSG DTT	with GSSG (0.5 mM) DTT (0.1 mM)
Reactivation	3000	637
Ammonium sulfate precipitation	16648	15590

Table 2. Purification of recombinant *Coprinus cinereus* peroxidase

Purification steps	total protein (mg)	total activity (U)	specific activity (U/mg)	yield[a] (%)	purification fold (X)	RZ (A_{404}/A_{280})
Solubilization in 6M urea	13.2					
Reactivation	13.2	39600	3000	100	1.0	
Ammonium sulfate precipitation	3.8	63261	16648	29	5.5	1.7
Sephacryl S-200	2.0	47087	23544	15	7.8	2.9

[a]Yield (%) estimated are based on total protein (mg)

Table 3. Comparison of CIP purified from *E. coli* with CIP isolated from *C. cinereus* UAMH 4103

CIP from *E. coli*						CIP from C. cinereus UAMH 4103[a]					
Purification steps	Total protein (mg)	Total activity (U)	specific activity (U/mg)	yield[b] (%)	RZ (A_{404}/A_{280})	Purification steps	Volume (ml)	Total activity (U)	U/ml	yield (%)	RZ (A_{405}/A_{280})
Solubilization in 6M urea	13.2					Culture supernatant	5150	115980	22.52	100.0	
Reactivation	13.2	39600	3000	100		Ultrafiltration	83	83332	1004	71.9	
Ammonium sulfate precipitation	3.8	63261	16648	29	1.7	DEAE pool	113	46895	415	40.4	1.01
Sephacryl S-200	2	47087	23544	15	2.9	Sephadex peak fraction	9	9240	1026.7	8.0	2.37
						FPLC peak fraction	1	280	280	0.2	2.50

[a]From Ikehata et al. (2005)[b]Yield (%) estimated are based on total protein (mg)

Table 4. Kinetic parameters of bacterially expressed CIP reacted with different hydrogen donors[a]

Substrates	K_m (mM)		V_{max} (μ mol/min/mg)		k_{cat} (min^{-1})		k_{cat}/K_m ($mM^{-1}min^{-1}$)	
	AH_2	H_2O_2	AH_2	H_2O_2	AH_2	H_2O_2	AH_2	H_2O_2
Phenol	8.3	0.87	5.76×10^{2}	5.39×10^{3}	2.36×10^{4}	2.21×10^{5}	2.84×10^{3}	2.53×10^{5}
MBTH	0.005	0.90	1.92×10^{2}	6.19×10^{2}	7.88×10^{3}	2.53×10^{4}	1.58×10^{6}	2.82×10^{4}

[a]The enzyme cocentrations used in the assay buffers with different hydrogen donors, Phenol and MBTH, were 4.36×10^{-6}mM, 1.35×10^{-5} mM ,respectively.

Table 5. Thermodynamics parameters of recombinant CIP were measured with differential scanning calorimetry (DSC) at pH 8.5.

parameters	values
T_m, ℃	48.0
ΔS, KJ mol^{-1} K^{-1}	1.09
ΔH_{cal}, KJ mol^{-1}	348.3

Table 6. Comparison of of recombinant CIP, HRP, AOPTP and SBP on thermostability.

Enzyme	T_m, ℃	Description
rCIP	48.0	pH 8.5, DSC
HRP[a]	71.4	pH 3.0, DSC
AOPTP[b]	74.6	pH 3.0, DSC
HRP[c]	62.2	pH 7.4, UV2450
SBP[d]	86.0	pH 7.0, far-UV CD

[a]From Pina et al., 2001 [b]From Rodriguez et al., 2002 [c]From Liu et al., 2006 [d]From Kizhakkedathu et al., 2002

Table 7. Secondary structure (%) determined by CD spectroscopy for intact and thermally treated CIP at pH 8.5

Protein state	α Helices			β Strands				
	Regular	Distorted	Total	Regular	Distorted	Total	β Turns	Disordered
Intact	26.3	20.2	46.5	5.5	6	11.5	20.8	24.9
55 ℃	20.1	13.7	33.8	5.2	7.6	12.8	24.1	33.4
80 ℃	6	9.5	15.5	20.4	11.7	32.1	22.7	35.4

Table 8. Absorption maxima of recombinant CIP and wt CIP

Enzymes	Absorption peaks λ, nm
r CIP[a]	404, 503, 644
wt CIP[b]	403, 505, 534, 649
wt CIP[c]	405, 504, 645

[a]pH 8.0; r CIP, recombinant CIP[b]From Smulevich et al. (1996)[c]From Anderson et al. (1991)